Nonlinear Dynamics **12:** 1–37, 1997.

Slow Periodic Crossing of a Pitchfork Bifurcation in an Oscillating System

G. J. M. MAREE
Department of Mathematics, Agricultural University, Dreijenlaan 4, 6703 HA Wageningen, The Netherlands

(Received: 16 March 1995; accepted: 28 May 1996)

Abstract. A study is made of the dynamics of oscillating systems with a slowly varying parameter. A slowly varying forcing periodically crosses a critical value corresponding to a pitchfork bifurcation. The instantaneous phase portrait exhibits a centre when the forcing does not exceed the critical value, and a saddle and two centres with an associated double homoclinic loop separatrix beyond this value. The aim of this study is to construct a Poincaré map in order to describe the dynamics of the system as it repeatedly crosses the bifurcation point. For that purpose averaging methods and asymptotic matching techniques connecting local solutions are applied. Given the initial state and the values of the parameters the properties of the Poincaré map can be studied. Both sensitive dependence on initial conditions and (quasi) periodicity are observed. Moreover, Lyapunov exponents are computed. The asymptotic expressions for the Poincaré map are compared with numerical solutions of the full system that includes small damping.

Key words: Chaos, dynamic bifurcations, matched asymptotic expansions, averaging, nonlinear oscillator, perturbation methods.

1. Introduction

In this study we consider the dynamics of a class of second order differential equations that describe damped oscillating systems with a slowly varying forcing function. The slow forcing periodically crosses a critical value. The phase portrait of the system changes qualitatively with time. Below the critical value this system exhibits a centre point in case the damping is neglected. On the other side of the bifurcation point a symmetric pair of centre points appears, while the original centre point has changed into a saddle point with an associated double homoclinic loop separatrix. In the reversed case we have a subcritical pitchfork bifurcation (see also [1]). The local transition behaviour is described by the second Painlevé transcendent. A prototype of system exhibiting this kind of behaviour is the nonlinear Mathieu equation. We will consider this system in which a small damping is allowed (turning the centre points into stable spiral points):

$$\frac{\mathrm{d}^2x}{\mathrm{d}t^2} + k\varepsilon\frac{\mathrm{d}x}{\mathrm{d}t} - x\cos(\varepsilon t) + 2x^3 = 0, \qquad 0 < \varepsilon \ll 1. \tag{1}$$

The bifurcation parameter slowly varies and periodically crosses a critical value corresponding to a pitchfork bifurcation. During half the forcing cycle the separatrices slowly grow and then slowly shrink, which implies that the two stable symmetric branches first turn away from the unstable equilibrium and then return until they disappear. At that moment the unstable equilibrium becomes stable.

The aim of this study is to construct a Poincaré map for one forcing period. This map approximates the dynamics of system (1) by monitoring the state of a motion once per forcing cycle. It is possible to predict which stable branch will be followed after each passage of the

bifurcation point on a time scale $O(1/\varepsilon)$, given the initial state and the values of the parameters. The initial values and the damping are chosen such that a motion outside the homoclinic separatrix loop does not occur. For the construction of the Poincaré map averaging methods and asymptotic matching techniques connecting local solutions are applied. Moreover, we use an important result concerning the second Painlevé equation stating that there is a connection between the integration constants of the asymptotic solution of the transition equation below criticality with the one above criticality [2].

The Poincaré map shows a complex dynamical behaviour. Depending on the initial state and the values of the parameter (quasi) periodic and chaotic orbits can be observed. We analyze the Lyapunov exponents that describe the structure of the "attractor" of the orbits. If one of these exponents is positive then the system has a strange attractor. The fractal dimension of this strange attractor follows from the conjecture of Kaplan and Yorke, see, e.g. [3]. Chaos in the system means that the sequence of selected lower and upper branches is irregular and exhibits sensitive dependence on initial conditions. Since the separatrix periodically disappears, Melnikov's method cannot be applied to this investigation.

In [4–6] the same system without damping is studied. It is shown that this model is qualitatively equivalent to familiar mechanical systems such as a dynamically buckled beam or a rotating plane pendulum. They obtain an asymptotic approximation by elliptic averaging and connect this solution to a separatrix boundary layer solution by point matching (patching). By introduction of a transition solution (the second Painlevé transcendent) the asymptotic matching technique as described by Eckhaus [7] can be applied. Our approach is extended to dissipative systems. Moreover, we prove the validity of the matched asymptotic approximations on a time scale $O(1/\varepsilon)$, and therefore also the validity of the approximating Poincaré map. We apply second order averaging methods as formulated by Verhulst [8], and Sanders and Verhulst [9]. Bourland and Haberman [10], and Neishtadt [11] study the problem of the crossing of a separatrix by nonlinear oscillations that correspond to a slowly varying potential which remains double-welled. Bosley and Kevorkian [12] consider transient resonance in very slowly varying oscillatory Hamiltonian systems for which the leading order frequency of the reduced system makes a continuous slow passage through zero. In [13] the phenomenon of instability of a mechanical system known as snap-through has been analyzed. Kaper and Wiggins [14] study the invariant structures in separatrix-swept regions of adiabatic planar Hamiltonian systems by using adiabatic Melnikov theory.

In Section 2 we formulate the model equation and describe the qualitative nature of its solution. In Section 3 the solution is approximated for intervals in which the solution is sufficiently bounded away above or below the bifurcation point. Moreover, the transition layer equation is analyzed and matching conditions for this local asymptotic solution are derived. In Section 4 we apply these matching conditions to the local asymptotic expansions and show that there is an overlap between the local (inner) solution of the second Painlevé equation and the other (outer) approximations. With this information a Poincaré map for one period of the forcing is constructed in Section 5. This map facilitates the analysis of the complex dynamics of the original system. In Section 6 we predict the behaviour of the system at the basis of the initial values and the parameter values. In Section 7 results, obtained from the analytical expressions for the map, are compared with the numerical solution of the full system.

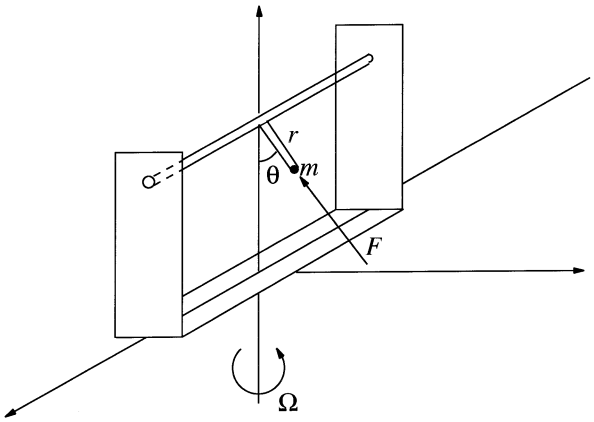

Figure 1a. Simple pendulum attached to a rotating rigid frame.

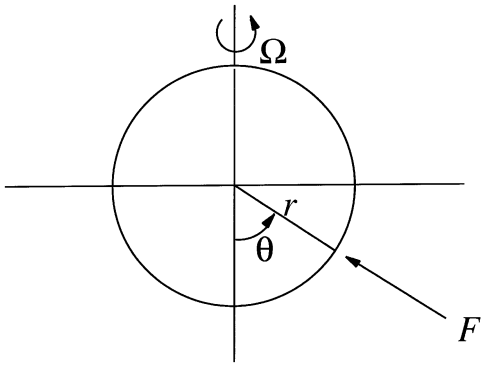

Figure 1b. A particle moving on a smooth, rotating circular wire.

2. The System and Its Qualitative Behaviour

We consider two examples of mechanical systems that exhibit the dynamical behaviour as described by Equation (1). First we discuss the pendulum of Figure 1a. It is attached to a rotating rigid frame and its deflection is measured by the angle θ with respect to the vertical.

This rigid frame is forced to rotate about a vertical axis at an angular velocity $\Omega(t)$. While the frame rotates, the simple pendulum oscillates. We assume that the pendulum consists of a mass m attached to a hinged weightless rod of length r. The forces acting on the mass m are the centrifugal force $m\Omega^2 r \sin\theta$, the gravitational force mg, and the reaction force F. We take moments about the centre of the circle along which the mass moves and equate their them tohis rate of change of the angular momentum of the particle about this centre. We obtain the following equation for the system without friction:

$$\frac{\mathrm{d}^2\theta}{\mathrm{d}\eta^2} + (1 - \Lambda\cos\theta)\sin\theta = 0, \tag{2}$$

where $\Lambda = \Omega^2((g/r)^{-1/2}\eta)r/g$ and the new independent variable is $\eta = (g/r)^{1/2}t$. For fixed Λ this system possesses one equilibrium if Λ is smaller than 1 and three equilibria if Λ is larger than 1. When we use the following modulations

$$\Lambda = 1 + \varepsilon\cos(\varepsilon^{3/2}\eta), \qquad \theta = 2\varepsilon^{1/2}x, \qquad \eta = \varepsilon^{-1/2}s \tag{3}$$

and expand for small ε, then Equation (2) becomes

$$\frac{\mathrm{d}^2x}{\mathrm{d}s^2} - x\cos(\varepsilon s) + 2x^3 + \cdots = 0, \tag{4}$$

where the dots represent terms of order ε. When we omit these higher order terms and assume a small damping of order ε in the original system (2) we obtain an equation of the form (1). The dynamics of this pendulum is equivalent to that of the motion of a particle on a smooth, rotating circular wire, as shown in Figure 1b.

In system (1) we define

$$G(t) = \cos(\varepsilon t). \tag{5}$$

For G fixed and smaller than the critical value

$$G_c = 0 \tag{6}$$

the system without friction contains one centre at the origin. When $G = G_c$ this unique equilibrium is still stable. For $G > G_c$ it becomes an unstable point of saddle point type. Moreover, the system then exhibits two centres at $(\pm\sqrt{(G/2)}, 0)$ as well as a double homoclinic loop separatrix. The transition from a stable line to a parabolic curve as G increases through G_c, is called a supercritical pitchfork bifurcation, whereas the transition in the reverse direction is a subcritical pitchfork bifurcation (see also Guckenheimer and Holmes [1]). For G fixed the energy integral of system (1) without friction is given by the Hamiltonian

$$H = \frac{1}{2}\left(\frac{\mathrm{d}x}{\mathrm{d}t}\right)^2 - \frac{1}{2}\,Gx^2 + \frac{1}{2}\,x^4. \tag{7}$$

In Figures 2 and 3 the pitchfork bifurcation is illustrated.

In Figure 4 numerical solutions of the complete system (1) are given. It shows the different aspects of the dynamic behaviour of the system. The impact of the damping and the sensitive dependence on the initial conditions are shown.

3. Local Asymptotic Expansions

In this section we construct local solutions to the initial value problem

$$\frac{\mathrm{d}^2x}{\mathrm{d}t^2} + k\varepsilon\frac{\mathrm{d}x}{\mathrm{d}t} - G(t)x + 2x^3 = 0, \qquad G(t) = \cos(\varepsilon t), \qquad 0 < \varepsilon \ll 1 \tag{8}$$

for different values of G and initial values near different stable branches. Note that $G(t)$ is 2π-periodic in $\tau = \varepsilon t$. First we will consider the initial value problem for an interval with $G(t) < 0$ and bounded away from zero, corresponding to initial conditions close to the outer equilibrium solution $x = 0$. Next, for $G > 0$ solutions to initial value problems are analyzed that are close to one of the two stable outer equilibrium solutions $x = \pm\sqrt{(G/2)}$. We will consider $O(\sqrt{\varepsilon})$-perturbations, because in that case the asymptotic expansion of a slowly varying equilibrium solution and the one of the perturbed averaged quantity break down simultaneously when the frequency of the nonlinear oscillator tends to zero (see, e.g., Haberman [15]). Finally, we obtain matching conditions for the local asymptotic solution describing the pitchfork bifurcation and show that the transition layer solution is a local approximation of the exact solution to the complete system.

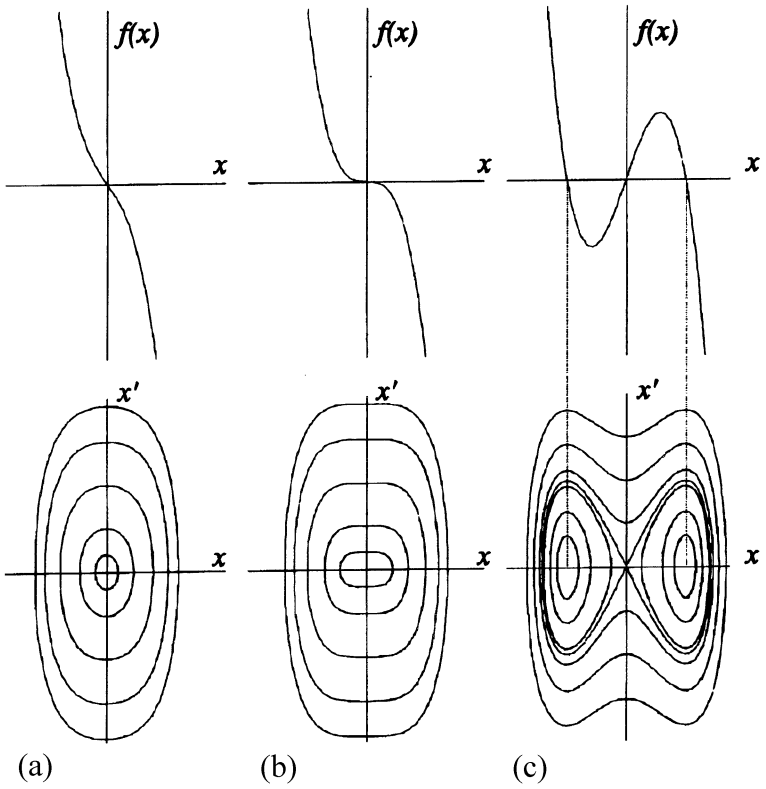

Figure 2. The graph of the function $f(x) = x(G - 2x^2)$ and the phase portrait of $\mathrm{d}^2x/\mathrm{d}t^2 - x(G - 2x^2) = 0$ for different values of G. (a) $G < G_c$, (b) $G = G_c$, (c) $G > G_c$.

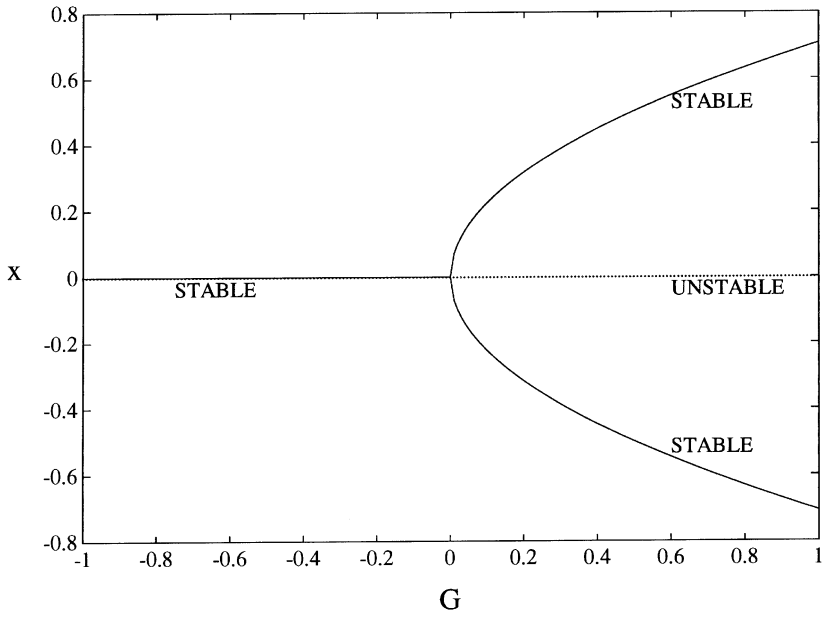

Figure 3. The branches of the limit solution for different values of G.

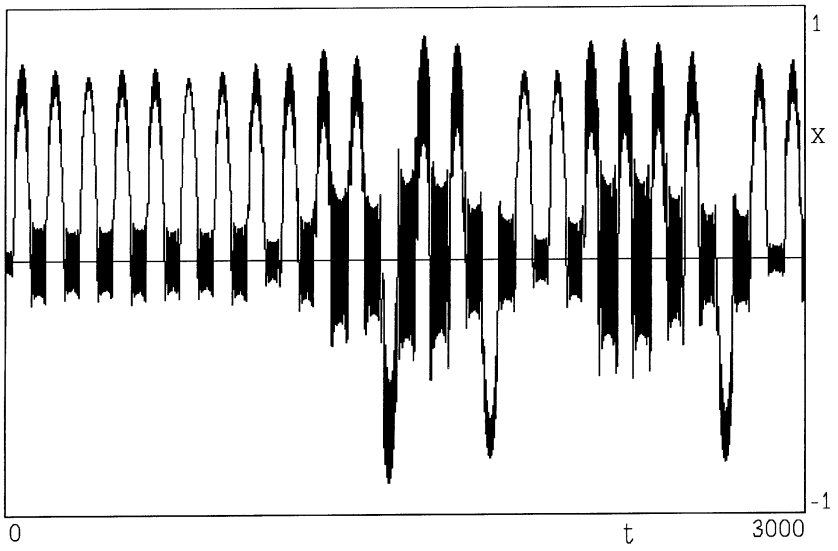

(a) $k = 0.1$, $\varepsilon = 0.05$, $x(t_0) = 0.04$

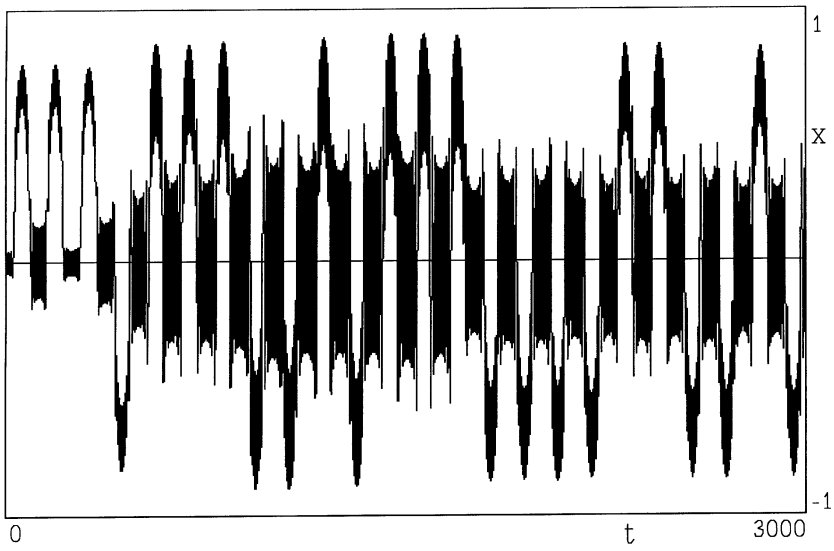

(b) $k = 0$, $\varepsilon = 0.05$, $x(t_0) = 0.04$

Figure 4. Numerical solutions of Equation (1) with $x'(t_0) = 0$ and $\cos(\varepsilon t_0) = -1$.

3.1. Asymptotic Expansion of the Solution below the Bifurcation Point

We consider perturbations of the equilibrium of the form

$$x(t) = \sqrt{\varepsilon}\, v(t) \tag{9}$$

and take as initial values for a certain time t_0

$$G(t_0) = -1, \qquad x(t_0) = \sqrt{\varepsilon}\, x_1, \qquad \frac{\mathrm{d}x}{\mathrm{d}t}\,(t_0) = \sqrt{\varepsilon}\, v_1. \tag{10}$$

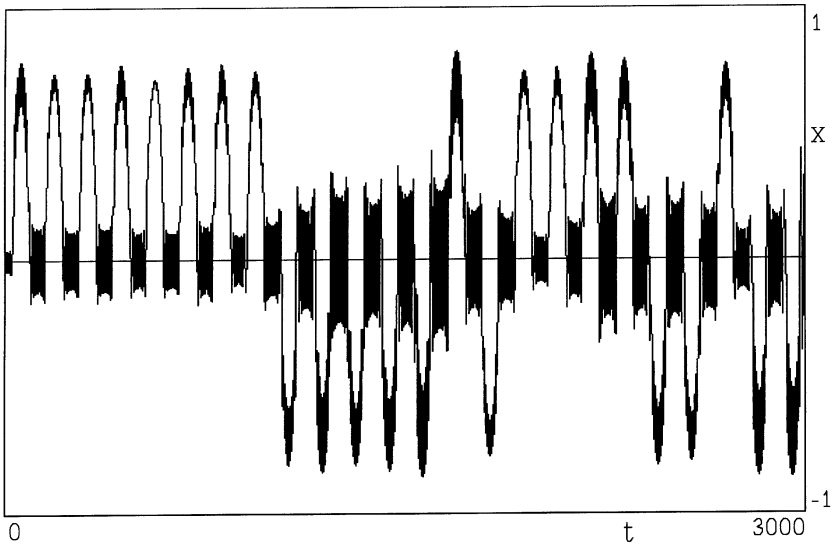

(c) $k = 0.1$, $\varepsilon = 0.05$, $x(t_0) = 0.039$

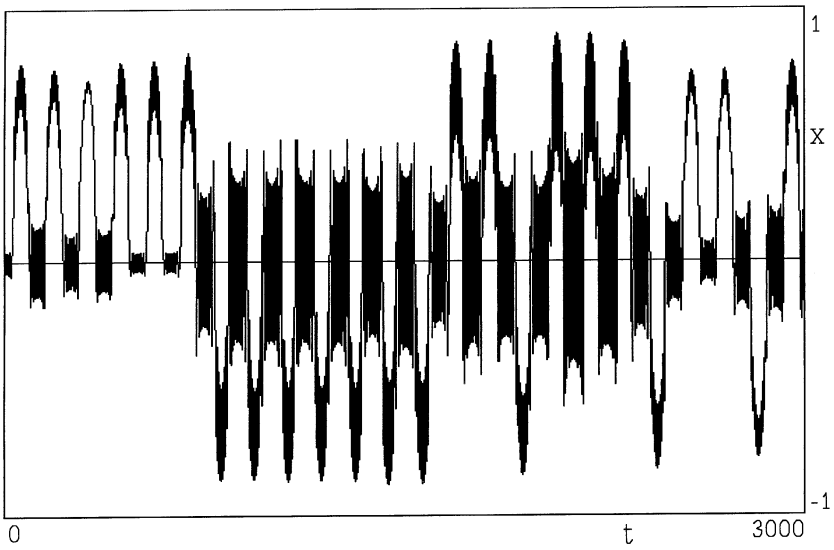

(d) $k = 0$, $\varepsilon = 0.05$, $x(t_0) = 0.039$

Figure 4. (Continued)

Substitution in (8) yields

$$\frac{\mathrm{d}^2 v}{\mathrm{d}t^2} + \omega_1^2(\tau)v = -k\varepsilon\frac{\mathrm{d}v}{\mathrm{d}t} - 2\varepsilon v^2 \tag{11}$$

with

$$\tau = \varepsilon t, \qquad \omega_1(\tau) = \sqrt{-\cos\tau} = \sqrt{-G}. \tag{12}$$

After the transformations

$$v = e^{-(1/2)k\varepsilon t}w := rw \tag{13}$$

and

$$w = \omega_1^{-1/2}(\tau)y \tag{14}$$

we obtain the following system

$$\frac{\mathrm{d}^2y}{\mathrm{d}t^2} + \omega_1^2(\tau)y \;=\; \varepsilon\left(-2\omega_1^{-1}(\tau)r^2y^3 + \omega_1^{-1}(\tau)\frac{\mathrm{d}y}{\mathrm{d}t}\,\frac{\mathrm{d}\omega_1}{\mathrm{d}\tau}\right)$$
$$+\,\varepsilon^2\left(\frac{1}{4}\,k^2y - \frac{3}{4}\,\omega_1^{-2}(\tau)y\left(\frac{\mathrm{d}\omega_1}{\mathrm{d}\tau}\right)^2 + \frac{1}{2}\,\omega_1^{-1}(\tau)y\frac{\mathrm{d}^2\omega_1}{\mathrm{d}\tau^2}\right), \tag{15a}$$

$$\frac{\mathrm{d}r}{\mathrm{d}t} = -\frac{1}{2}\,k\varepsilon r, \tag{15b}$$

with

$$\frac{\mathrm{d}\omega_1}{\mathrm{d}\tau} = \frac{\sin\tau}{2\sqrt{-\cos\tau}}\,, \tag{16a}$$

$$\frac{\mathrm{d}^2\omega_1}{\mathrm{d}\tau^2} = -\frac{1}{2}\,\sqrt{-\cos\tau} - \frac{\sin^2\tau}{4\sqrt{-\cos\tau}}\,. \tag{16b}$$

and

$$G = \cos\tau < 0. \tag{16c}$$

REMARK. When for $t \geq 0$ the inequalities $0 < a < \omega(\varepsilon t) < b$ and $|\mathrm{d}\omega/\mathrm{d}(\varepsilon t)| < c$ hold with a, b and c arbitrary constants independent of ε, then the ratio of the energy and its frequency (the adiabatic invariant of a harmonic oscillator) is conserved with accuracy $O(\varepsilon)$ on a time scale $O(1/\varepsilon)$. Therefore, transformation (14) can be regarded as an "adiabatic transformation". Equation (13) shows that the damping causes an exponential decay.

We now carry out the transformation

$$\frac{\mathrm{d}y}{\mathrm{d}t} = \omega_1(\tau)u, \tag{17a}$$

$$\frac{\mathrm{d}u}{\mathrm{d}t} = \frac{1}{\omega_1(\tau)}\,\frac{\mathrm{d}^2y}{\mathrm{d}t^2} - \frac{\varepsilon}{\omega_1(\tau)}\,\frac{\mathrm{d}\omega_1}{\mathrm{d}\tau}\,u \tag{17b}$$

and introduce polar coordinates

$$y = r_1\sin\phi_1, \qquad u = r_1\cos\phi_1 \tag{18a}$$

with values at t_0

$$y(t_0) = r_{10}\sin\phi_{10}, \qquad u(t_0) = r_{10}\cos\phi_{10}. \tag{18b}$$

These transformations are carried out in order to obtain a system to which we can apply averaging methods (see, e.g., Sanders and Verhulst [9]). Next, we make the transformation

$$\tau_1 = \int_{\varepsilon t_0}^{\tau} \frac{\omega_1(\tau)\,\mathrm{d}\tau}{\varepsilon} = \frac{1}{2}\,B_{\tau-\varepsilon t_0}\left(\frac{1}{2}\,,\frac{3}{4}\right) \tag{19}$$

with $B_x(a,b)$ the incomplete Beta function as defined in [16].

In fact, we use the method of multiple scales with a slow time εt and a fast time τ_1. Now we set

$$\psi_1 = \phi_1 - \tau_1, \tag{20}$$

so we finally arrive at the following initial value problem with $\tau_1 = 0$ for $t = t_0$:

$$\frac{\mathrm{d}r}{\mathrm{d}\tau_1} = \frac{-k\varepsilon}{2\omega_1(\tau)}, \qquad r(0) = e^{-k\varepsilon t_0/2}, \tag{21a}$$

$$\begin{aligned}\frac{\mathrm{d}r_1}{\mathrm{d}\tau_1} = {} & \frac{\varepsilon}{\omega_1^3(\tau)}\Big(-2r^2r_1^3\sin^3(\psi_1+\tau_1)\cos(\psi_1+\tau_1) \\ & + \frac{1}{4}\,k^2\varepsilon r_1\omega_1(\tau)\sin(\psi_1+\tau_1)\cos(\psi_1+\tau_1)\Big) \\ & + \frac{\varepsilon^2}{\omega_1^4(\tau)}\left(-\frac{3}{4}\,r_1\left(\frac{\mathrm{d}\omega_1}{\mathrm{d}\tau}\right)^2\sin(\psi_1+\tau_1)\cos(\psi_1+\tau_1)\right. \\ & \left. + \frac{1}{2}\,\omega_1(\tau)r_1\frac{\mathrm{d}^2\omega_1}{\mathrm{d}\tau^2}\,\sin(\psi_1+\tau_1)\cos(\psi_1+\tau_1)\right), \qquad r_1(0) = r_{10}\end{aligned} \tag{21b}$$

$$\begin{aligned}\frac{\mathrm{d}\psi_1}{\mathrm{d}\tau_1} = {} & \frac{\varepsilon}{\omega_1^3(\tau)}\left(2r^2r_1^2\sin^4(\psi_1+\tau_1) - \frac{1}{4}\,k^2\varepsilon\omega_1(\tau)\sin^2(\psi_1+\tau_1)\right) \\ & + \frac{\varepsilon^2}{\omega_1^4(\tau)}\left(\frac{3}{4}\left(\frac{\mathrm{d}\omega_1}{\mathrm{d}\tau}\right)^2\sin^2(\psi_1+\tau_1) - \frac{1}{2}\,\omega_1(\tau)\frac{\mathrm{d}^2\omega_1}{\mathrm{d}\tau^2}\sin^2(\psi_1+\tau_1)\right), \\ & \psi_1(0) = \phi_{10}.\end{aligned} \tag{21c}$$

The phase shift (20) is necessary in order to get a system that can be averaged over a certain fixed period of the fast time τ_1. From (12) and (19) we conclude that $\omega_1(\tau) = 0$ for $\tau = \tau^*$ or $\tau_1 = \tau_1^*$ with

$$\tau^* = \varepsilon t_0 + \frac{\pi}{2}, \qquad \tau_1^* = \frac{B(1/2,3/4)}{2\varepsilon}, \tag{22}$$

where $B(z,w)$ is the Beta function as defined in [16]. In [17] an approximation theorem has been proven for $\tau_1 \in [0,(1/2)B(1/2,3/4)\varepsilon^{-1} - \delta_1^{-1}(\varepsilon)]$ – so for $\tau \in [\varepsilon t_0, \varepsilon t_0 + (\pi/2) - \varepsilon^{2/3}\delta_2^{-2/3}(\varepsilon)]$ or $G \in [-1, -\varepsilon^{2/3}\delta_3^{-2/3}(\varepsilon)]$ – with δ_1, δ_2 and δ_3 positive asymptotic order functions of order $o(1)$. This theorem establishes the validity of an asymptotic expansion of the solution of (8) in the neighbourhood of $x_0 = 0$ for $G = \cos\tau < 0$ and $\varepsilon^{2/3} = o(G)$. For the present problem the theorem is stated as follows.

THEOREM 3.1. *For $-1 < G < 0$ and $\varepsilon^{2/3} = o(G)$ the solution of (8) has the following expansion*

$$x(t) = \sqrt{\varepsilon}\,r_a r_{1a}\omega_1^{-1/2}(\tau)\sin(\tau_1 + \psi_{1a}) + o(\sqrt{\varepsilon}\,\omega_1^{-1/2}(\tau)) \tag{23}$$

with (r_{1a}, ψ_{1a}, r_a) the solution of the system with initial values at $\tau_1 = 0$

$$\frac{\mathrm{d}r_{1a}}{\mathrm{d}\tau_1} = 0, \qquad r_{1a}(0) = r_{10}, \tag{24a}$$

$$\frac{\mathrm{d}\psi_{1a}}{\mathrm{d}\tau_1} = \frac{\varepsilon}{\omega_1^3(\tau)}\left(\frac{3}{4}\, r_a^2 r_{1a}^2 - \frac{1}{8}\, k^2 \varepsilon \omega_1(\tau)\right), \qquad \psi_{1a}(0) = \phi_{10}, \tag{24b}$$

$$\frac{\mathrm{d}r_a}{\mathrm{d}\tau_1} = \frac{-k\varepsilon r_a}{2\omega_1(\tau)}, \qquad r_a(0) = e^{-k\varepsilon t_0/2}. \tag{24c}$$

□

Problems arise when the angular velocity $\omega_1(\tau)$ tends to zero. So there is a boundary layer behaviour in the neighbourhood of $G = 0$. When G crosses zero from below a supercritical pitchfork bifurcation takes place. Approximations for the supercritical times are therefore $t = (3\pi/2 + 2\pi n)/\varepsilon$, $n \in \mathbb{N}$.

REMARK. The critical time τ_1^* as defined in (22) is obtained by computing

$$I = \int_0^{\pi/2} \sqrt{\cos(s)}\, \mathrm{d}s. \tag{25}$$

It can be shown that

$$I = \frac{1}{2}\, B\left(\frac{1}{2}, \frac{3}{4}\right) = \frac{\Gamma(1/2)\Gamma(3/4)}{2\Gamma(5/4)} = \frac{2\sqrt{2}\cdot\pi\sqrt{\pi}}{\Gamma(1/4)^2} = 1.1981, \tag{26a}$$

or alternatively

$$I = 2\sqrt{2}\, E\left(\frac{1}{2}\right) - \sqrt{2}\, K\left(\frac{1}{2}\right) = 1.1981 \tag{26b}$$

with Γ the gamma function and K and E the complete elliptic integrals of respectively the first and second kind.

3.2. Asymptotic Expansion of the Solution above the Bifurcation Point

We analyze the solution to the initial value problem (8) for $G \geq \delta(\varepsilon) > 0$ close to one of the two stable outer equilibrium solutions $x_{\pm 1} = \pm\sqrt{(G/2)}$. Because of the symmetry of the problem it is sufficient to consider the perturbations of one of the equilibria of the undamped system with fixed forcing. We choose $x = x_1 = \sqrt{(G/2)}$. We rewrite (8) in order to analyze a slowly varying equilibrium solution $x_{1sv}(\tau)$:

$$\frac{\mathrm{d}^2 x}{\mathrm{d}t^2} = \varepsilon^2 \frac{\mathrm{d}^2 x}{\mathrm{d}\tau^2} = -k\varepsilon^2 \frac{\mathrm{d}x}{\mathrm{d}\tau} + g(x, \tau) \tag{27}$$

with

$$\tau = \varepsilon t \quad \text{and} \quad g(x, \tau) = x(\cos\tau - 2x^2). \tag{28}$$

Assuming that the derivatives in (27) are small, we obtain a slowly varying equilibrium solution for $G = \cos\tau > 0$ by perturbing the dependent variable at $x_1(\tau) = \sqrt{(\cos\tau/2)}$. Because $g(x_1, \tau) = 0$, we can use the Taylor series of $g(x, \tau)$ at $x = x_1(\tau)$. In this way we

obtain an asymptotic expansion for the slowly varying equilibrium solution of (27):

$$x_{1sv}(\tau) = \sqrt{\frac{\cos\tau}{2}} + \varepsilon^2 \left(\frac{1}{16}\, k \sin\tau \left(\frac{\cos\tau}{2} \right)^{-3/2} + \frac{1}{2} \left(\frac{\cos\tau}{2} \right)^{1/2} + \frac{1}{64}\, \sin^2\tau \left(\frac{\cos\tau}{2} \right)^{-5/2} \right) + \cdots \tag{29}$$

For a solution that holds in a $\sqrt{\varepsilon}$-neighbourhood of this slowly varying solution we write:

$$x(t) = x_{1sv}(\tau) + \sqrt{\varepsilon}\, v(t). \tag{30}$$

Furthermore, we assume that the solution takes the following values for $t = t_1 = t_0 + (\pi/\varepsilon)$ (so for $\tau_0 = \varepsilon t_0 + \pi$) with t_0 as defined in Section 3.1

$$x(t_1) = x_1(\tau_0) + \sqrt{\varepsilon}\, x_{10}, \tag{31a}$$

$$\frac{\mathrm{d}x}{\mathrm{d}t}\,(t_1) = \frac{\mathrm{d}x_1}{\mathrm{d}t}\,(\tau_0) + \sqrt{\varepsilon}\, y_{10}, \tag{31b}$$

$$G(t_1) = 1. \tag{31c}$$

Substitution in (8) yields

$$\frac{\mathrm{d}^2 v}{\mathrm{d}t^2} + \omega_2^2(\tau) v = -\sqrt{\varepsilon}\, 6v^2 x_{1sv}(\tau) - \varepsilon \left(k \frac{\mathrm{d}v}{\mathrm{d}t} + 2v^3 \right) \tag{32}$$

with

$$\omega_2^2(\tau) = 6x_{1sv}^2(\tau) - \cos\tau. \tag{33}$$

After the transformation

$$v = e^{-(1/2)k\varepsilon t} w := rw \tag{34}$$

and

$$w = \omega_2^{-1/2}(\tau) y \tag{35}$$

we obtain the following system

$$\frac{\mathrm{d}^2 y}{\mathrm{d}t^2} + \omega_2^2(\tau) y = \sqrt{\varepsilon} \left(-6\omega_2^{-1/2}(\tau) r y^2 x_{1sv}) + \varepsilon(-2\omega_2^{-1}(\tau) r^2 y^3 + \omega_2^{-1}(\tau) \frac{\mathrm{d}y}{\mathrm{d}t}\, \frac{\mathrm{d}\omega_2}{\mathrm{d}t} \right) + \varepsilon^2 \left(\frac{1}{4}\, k^2 y - \frac{3}{4}\, \omega_2^{-2}(\tau) y \left(\frac{\mathrm{d}\omega_2}{\mathrm{d}\tau} \right)^2 + \frac{1}{2}\, \omega_2^{-1}(\tau) y \frac{\mathrm{d}^2\omega_2}{\mathrm{d}\tau^2} \right), \tag{36a}$$

$$\frac{\mathrm{d}r}{\mathrm{d}t} = -\frac{1}{2}\, k\varepsilon r. \tag{36b}$$

In the same way as in Section 3.1 we now carry out the transformation

$$\frac{\mathrm{d}y}{\mathrm{d}t} = \omega_2(\tau) u, \tag{37a}$$

$$\frac{\mathrm{d}u}{\mathrm{d}t} = \frac{1}{\omega_2^2(\tau)}\,\frac{\mathrm{d}^2y}{\mathrm{d}t^2} - \frac{\varepsilon}{\omega_2(\tau)}\,\frac{\mathrm{d}\omega_2}{\mathrm{d}\tau}\,u \tag{37b}$$

and introduce polar coordinates

$$y = r_2\cos\phi_2, \qquad u = -r_2\sin\phi_2 \tag{38a}$$

with values at t_1

$$y(t_1) = r_{20}\cos\phi_{20}, \qquad u(t_1) = -r_{20}\sin\phi_{20}. \tag{38b}$$

Next, we make the transformation

$$\tau_2 = \int_{\tau}^{\varepsilon t_1} \frac{\omega_2(\tau)}{\varepsilon}\,\mathrm{d}\tau \tag{39}$$

and set

$$\psi_2 = \phi_2 + \tau_2. \tag{40}$$

Thus, we finally arrive at the following system

$$\frac{\mathrm{d}r}{\mathrm{d}\tau_2} = \frac{k\varepsilon r}{2\omega_2(\tau)}\,, \qquad r(\varepsilon t_1) = e^{-k\varepsilon t_1/2}, \tag{41a}$$

$$\begin{aligned}
\frac{\mathrm{d}r_2}{\mathrm{d}\tau_2} \;=\; & -\sqrt{\varepsilon}\,(6\omega_2^{-5/2}(\tau)rr_2^2\cos^2(\psi_2-\tau_2)\sin(\psi_2-\tau_2)x_{1sv}(\tau)) \\
& -\varepsilon\omega_2^{-3}(\tau)\bigg(-\frac{1}{4}\,k^2\varepsilon\omega_2(\tau)r_2\cos(\psi_2-\tau_2)\sin(\psi_2-\tau_2) \\
& +2r^2r_2^3\cos^3(\psi_2-\tau_2)\sin(\psi_2-\tau_2)\bigg) \\
& -\varepsilon^2\omega_2^{-4}(\tau)\left(\frac{3}{4}\,r_2\cos(\psi_2-\tau_2)\sin(\psi_2-\tau_2)\left(\frac{\mathrm{d}\omega_2}{\mathrm{d}\tau}\right)^2\right. \\
& \left.+\;\frac{1}{2}\,\omega_2(\tau)r_2\cos(\psi_2-\tau_2)\sin(\psi_2-\tau_2)\frac{\mathrm{d}^2\omega_2}{\mathrm{d}\tau^2}\right), \qquad r_2(\varepsilon t_1) = r_{20}.
\end{aligned} \tag{41b}$$

$$\begin{aligned}
\frac{\mathrm{d}\psi_2}{\mathrm{d}\tau_2} \;=\; & -\sqrt{\varepsilon}\,(6\omega_2^{-5/2}(\tau)rr_2^2\cos^3(\psi_2-\tau_2)x_{1sv}(\tau)) \\
& -\varepsilon\left(-\frac{1}{4}\,k^2\varepsilon\omega_2^{-2}(\tau)\cos^2(\psi_2-\tau_2)+2\omega_2^{-3}(\tau)r^2r_2^2\cos^4(\psi_2-\tau_2)\right) \\
& -\varepsilon^2\left(\frac{3}{4}\,\omega_2^{-4}(\tau)\cos^2(\psi_2-\tau_2)\left(\frac{\mathrm{d}\omega_2}{\mathrm{d}\tau}\right)^2+\frac{1}{2}\,\omega_2^{-3}(\tau)\cos^2(\psi_2-\tau_2)\frac{\mathrm{d}^2\omega_2}{\mathrm{d}\tau^2}\right), \\
& \psi_2(\varepsilon t_1) = \phi_{20}.
\end{aligned} \tag{41c}$$

We consider

$$0 < \delta_1(\varepsilon) \leq G = \cos\tau \leq 1 \tag{42a}$$

with

$$\varepsilon^{2/3} = o(\delta_1(\varepsilon)) \tag{42b}$$

and obtain the following approximations

$$x_{1sv}(\tau) = \sqrt{\cos\tau/2} + O(\varepsilon^2(\cos\tau)^{-5/2}), \tag{43a}$$

$$\omega_2(\tau) = \sqrt{2\cos\tau}\,(1 + O(\varepsilon^2(\cos\tau)^{-3})). \tag{43b}$$

In [17] a "second order" approximation theorem has been proven. An estimate of $O(\varepsilon(\cos\tau)^{-3/2})$ has been obtained taking into account both the $O(\varepsilon^{1/2}(\cos\tau)^{-3/4})$ terms and the $O(\varepsilon(\cos\tau)^{-3/2})$ terms of (41). Note the difference with Section 3.1, due to the fact that we are now near a non-trivial equilibrium branch. Moreover, we remark that (42) is valid when

$$\tau_2 \in \left[0, \sqrt{2}\frac{B(1/2,3/4)}{\varepsilon} - \delta_2^{-1}(\varepsilon)\right] \quad \text{with} \quad \delta_2 = o(1). \tag{44}$$

We now formulate the following approximation result.

THEOREM 3.2. *For $0 < \delta_1(\varepsilon) \leq G = \cos\tau \leq 1$ with $\varepsilon^{2/3} = o(\delta_1(\varepsilon))$ – so for $\delta_3(\varepsilon) \leq \omega_2(\tau) \leq \delta_4(\varepsilon)$ with $\varepsilon^{1/3} = o(\delta_3(\varepsilon))$ and $\delta_4(\varepsilon) = O(1)$ – the solution of (8) has the following expansion*

$$x(t) = \sqrt{\cos\tau/2} + \sqrt{\varepsilon}\, r_{2a} e^{-(1/2)k\varepsilon t}\omega_2^{-1/2}(\tau)\cos(\psi_{2a} - \tau_2) + o(\sqrt{\varepsilon}\,\omega_2^{-1/2}(\tau)), \tag{45}$$

with (r_{2a}, ψ_{2a}) the solution of the system

$$\frac{\mathrm{d}r_{2a}}{\mathrm{d}\tau_2} = 0, \qquad r_{2a}(t_1) = r_{20}, \tag{46a}$$

$$\frac{\mathrm{d}\psi_{2a}}{\mathrm{d}\tau_2} = -\varepsilon\left(\frac{-k^2\varepsilon}{16\cos\tau} + \frac{3e^{-k\varepsilon t}r_{2a}^2}{4(2\cos\tau)^{3/2}} - \frac{15e^{-k\varepsilon t}r_{2a}^2}{4(2\cos\tau)^{3/2}}\right), \qquad \psi_{2a}(t_1) = \phi_{20}, \tag{46b}$$

□

Finally we remark that in the case without damping (32) is a Hamiltonian system. After the transformations

$$v = r\cos\phi, \qquad \frac{\mathrm{d}v}{\mathrm{d}t} = -\omega_2(\tau)r\sin\phi, \quad \text{and} \quad p = r^2\omega_2(\tau)$$

we obtain a Hamiltonian of the following form

$$\begin{aligned} H \;=\; & \omega_2(\tau)p + \sqrt{\varepsilon}\,(3p^{3/2}\omega_2^{-3/2}(\tau)x_{1sv}(\tau)\cos\phi + p^{3/2}\omega_2^{-3/2}(\tau)x_{1sv}(\tau)\cos 3\phi) \\ & + \varepsilon\left(\frac{3}{8}\,p^2\omega_2^{-2}(\tau) + \frac{1}{2}\,p^2\omega_2^{-2}(\tau)\cos 2\phi\right. \\ & \left. + \frac{1}{8}\,p^2\omega_2^{-2}(\tau)\cos 4\phi - \frac{1}{2}\,p^2\omega_2^{-1}(\tau)\frac{\mathrm{d}\omega_2}{\mathrm{d}\tau}\,\sin 2\phi\right). \end{aligned} \tag{47}$$

3.3. THE TRANSITION LAYER EQUATION AND MATCHING CONDITIONS

In order to obtain matching conditions for the local asymptotic solution describing the pitchfork bifurcation we determine the asymptotic development of x when G is in the neighbourhood of $G_0 = 0$. We assumed that near $G = \cos\tau = 0$ and $x = 0$

$$g(x,\tau) = x(\cos\tau - 2x^2) = -\frac{1}{2}\,x(x - \sqrt{\cos\tau/2})(x + \sqrt{\cos\tau/2}). \tag{48}$$

Setting

$$t = t_0 + \frac{\pi}{2\varepsilon} + \varepsilon^{v-1}z \tag{49a}$$

or

$$G = \varepsilon^v z \tag{49b}$$

we obtain the following approximations for the τ-dependent terms in the asymptotic expansions (23) and (45):

$$r = \exp\left(-\frac{1}{2}\,k\varepsilon\left(t_0 + \frac{\pi}{2\varepsilon}\right)\right) + \cdots, \tag{50a}$$

$$\omega_1^2(\tau) = -z\varepsilon^v, \tag{50b}$$

$$x_{1sv}(\tau) = \left(\frac{z}{2}\right)^{1/2}\varepsilon^{v/2} + \frac{1}{64}\left(\frac{z}{2}\right)^{-5/2}\varepsilon^{2-5v/2} + \cdots + \frac{k}{16}\left(\frac{z}{2}\right)^{-3/2}\varepsilon^{2-3v/2} + \cdots, \tag{50c}$$

$$\omega_2^2(\tau) = 2z\varepsilon^v + \frac{3}{16}\left(\frac{z}{2}\right)^{-2}\varepsilon^{2-2v} + \cdots, \tag{50d}$$

$$r_{1a} = r_{10}, \tag{50e}$$

$$r_{2a} = r_{20}, \tag{50f}$$

$$\tau_1 = \int_{\varepsilon t_0}^{\varepsilon t_0 + \pi/2 + \varepsilon^v z} \frac{\sqrt{-\cos\tau}}{\varepsilon}\,\mathrm{d}\tau = \frac{B(1/2,3/4)}{2\varepsilon} - \frac{2}{3}\,(-z)^{3/2}\varepsilon^{3v/2-1} + \cdots, \tag{50g}$$

$$\begin{aligned}\tau_2 &= \int_{\varepsilon t_0 + \pi/2 + \varepsilon^v z}^{\varepsilon t_1} \frac{\sqrt{2\cos\tau}\,\mathrm{d}\tau}{\varepsilon} + \cdots \\ &= \frac{\sqrt{2}\,B(1/2,3/4)}{2\varepsilon} - \frac{2\sqrt{2}}{3}\,(z)^{3/2}\varepsilon^{3v/2-1} + \cdots,\end{aligned} \tag{50h}$$

$$\begin{aligned}\psi_{1a} &= \int_{\varepsilon t_0}^{\varepsilon t_0 + \pi/2 + \varepsilon^v z} \left(\frac{-3r_{10}^2 e^{-k\tau}}{4\cos\tau} - \frac{k^2\varepsilon}{8\sqrt{-\cos\tau}}\right)\mathrm{d}\tau \\ &= -\frac{3}{4}\,r_{10}^2 e^{-k\varepsilon t_0}\left(e^{-k\pi/2}\left(\ln(-z) + \ln\left(\frac{\varepsilon^v}{2}\right)\right) - k\int_0^{\pi/2}\ln\left(\frac{1+\sin y}{\cos y}\right)e^{-ky}\,\mathrm{d}y\right) \\ &\quad - \frac{\varepsilon k^2\sqrt{2}\,K(1/2)}{8} + \phi_{10} + \cdots,\end{aligned} \tag{50i}$$

$$\psi_{2a} = \int_{\varepsilon t_0+\pi/2+\varepsilon^v z}^{\varepsilon t_1} \left(\frac{-3r_{20}^2\varepsilon^{-k\tau}}{2\cos\tau} + \frac{k^2\varepsilon\sqrt{2}}{16\sqrt{\cos\tau}} \right) \mathrm{d}\tau$$

$$= -\frac{3}{2}\, r_{20}^2\varepsilon^{-k\varepsilon t_0} \left(e^{-k\pi/2} \left(\ln(z) + \ln\left(\frac{\varepsilon^v}{2}\right)\right) + k \int_{\pi/2}^{\pi} \ln\left(\frac{\sin y - 1}{\cos y}\right) e^{-ky}\, \mathrm{d}y \right)$$

$$+ \frac{\varepsilon k^2 K(1/2)}{8} + \phi_{20} + \cdots \tag{50j}$$

with K the complete elliptic integral of the first kind. Consequently, near the bifurcation point the outer solutions (23) and (45) behave asymptotically as

$$x \sim r_{10}e^{-(1/2)k\varepsilon(t_0+\pi/(2\varepsilon))}(-z)^{-1/4}\varepsilon^{1/2-v/4}$$

$$\times \sin\left(\frac{2}{3}\,(-z)^{3/2}\varepsilon^{3v/2-1} + \frac{3}{4}\, r_{10}^2 e^{-k\varepsilon t_0} \left(e^{-k\pi/2}(\ln(-z) + v\ln\varepsilon) \right.\right.$$

$$\left.\left. - k\int_0^{\pi/2} \ln\left(\frac{1+\sin y}{\cos y}\right) e^{-ky}\, \mathrm{d}y \right) + \psi_{10} + \cdots \right) + \cdots \quad \text{if} \quad z \to -\infty, \tag{51a}$$

$$x \sim \left(\frac{z}{2}\right)^{1/2}\varepsilon^{v/2} + \frac{1}{64}\left(\frac{z}{2}\right)^{-5/2}\varepsilon^{2-5v/2} + \cdots + \frac{k}{16}\left(\frac{z}{2}\right)^{-3/2}\varepsilon^{3/2-3v/2} + \cdots$$

$$+ r_{20}e^{-(1/2)k\varepsilon(t_0+\pi/(2\varepsilon))} \left(2z\varepsilon^v + \frac{3}{16}\left(\frac{z}{2}\right)^{-2}\varepsilon^{2-2v} + \cdots \right)^{-1/4} \varepsilon^{1/2}$$

$$\times \cos\left(\frac{2\sqrt{2}}{3}\,(z)^{3/2}\varepsilon^{3v/2-1} - \frac{3}{2}\, r_{20}^2 e^{-k\varepsilon t_0} \left(e^{-k\pi/2}(\ln(z) + v\ln\varepsilon) \right.\right.$$

$$\left.\left. + k\int_{\pi/2}^{\pi} \ln\left(\frac{\sin y - 1}{\cos y}\right) e^{-ky}\, \mathrm{d}y \right) + \psi_{20} + \cdots \right) + \cdots \quad \text{if} \quad z \to \infty, \tag{51b}$$

where ψ_{10} and ψ_{20} are constants determined by the initial conditions and the dots stand for higher order ε-terms or for terms that are $o(|z|^{-1/4})$.

From the expansion (51) it is seen that the outer expansion breaks down if $v = 2/3$. It implies that the transition layer (inner) equation follows from the scaling

$$x = \varepsilon^{1/3}y(z). \tag{52}$$

There is a significant degeneration of the differential Equation (8) that describes the transition behaviour for $G = \varepsilon^{2/3}z$ and $x = \varepsilon^{1/3}y(z)$. This degeneration is represented by the second Painlevé equation:

$$\frac{\mathrm{d}^2y}{\mathrm{d}z^2} = yz - 2y^3. \tag{53}$$

We refer to [17] for more details about this equation.

4. Matching Conditions for the Local Asymptotic Expansions and Their Interrelations

At the time that a pitchfork bifurcation is expected Equation (53) holds. Its solution must match the outer solutions as given by (51a) and (51b) with $v = 2/3$

$$y \sim \gamma(-z)^{-1/4} \sin\left\{\frac{2}{3}\,(-z)^{3/2} + \frac{3}{4}\,\gamma^2 \ln(-z) + \xi_{10}\right\} + o((-z)^{-1/4}) \quad \text{as} \quad z \to -\infty, \tag{54a}$$

$$y \sim \left(\frac{z}{2}\right)^{1/2} + \beta(2z)^{-1/4} \cos\left\{\frac{2\sqrt{2}}{3}\,z^{3/2} - \frac{3}{2}\,\beta^2 \ln(z) + \xi_{20}\right\} + o(z^{-1/4}) \quad \text{as} \quad z \to \infty, \tag{54b}$$

where

$$\gamma = r_{10} e^{-(1/2)k\varepsilon(t_0 + (\pi/2\varepsilon))}, \tag{54c}$$

$$\beta = r_{20} e^{-(1/2)k\varepsilon(t_0 + (\pi/2\varepsilon))}, \tag{54d}$$

$$\xi_{10} = \frac{-B(1/2, 3/4)}{2\varepsilon} + \frac{3}{4}\,r_{10}^2 e^{-k\varepsilon t_0} \times \left(e^{-k\pi/2}\left(\ln\frac{\varepsilon^{2/3}}{2}\right) - k\int_0^{\pi/2} \ln\left(\frac{1+\sin y}{\cos y}\right) e^{-ky}\,\mathrm{d}y\right) - \varphi_{10} + \pi, \tag{54e}$$

$$\xi_{20} = \frac{-\sqrt{2}\,B(1/2, 3/4)}{2\varepsilon} - \frac{3}{2}\,r_{20}^2 e^{-k\varepsilon t_0} \times \left(e^{-k\pi/2}\left(\ln\frac{\varepsilon^{2/3}}{2}\right) + k\int_{\pi/2}^{\pi} \ln\left(\frac{\sin y - 1}{\cos y}\right) e^{-ky}\,\mathrm{d}y\right) + \varphi_{20}. \tag{54f}$$

The pitchfork matching condition after passage of the bifurcation point when the solution remains near the stable outer solution $x = x_1$, is represented by (54b). When the solution remains near the other stable outer equilibrium solution $x = x_{-1} = -\sqrt{(G/2)}$ this matching condition is obtained by reflecting (54b) with respect to the z-axis. The asymptotic conditions are automatically fulfilled by (53).

From an approximation theorem formulated by Marée ([17], Theorem 5.2) and the extension theorem [7] it follows that the domain of validity of the local Painlevé approximation can be extended forward and backward to $G \in [-\varepsilon^{2/3}\delta_e^{-1}(\varepsilon), \varepsilon^{2/3}\delta_e^{-1}(\varepsilon)]$ with $\delta_e(\varepsilon) = o(1)$. Thus overlap with the domains, where outer approximations are valid, is ensured and so the integration constants can be matched. In [2] it is shown that there is a connection between the behaviour of solutions of the second Painlevé transcendent (53) for $z \to -\infty$ with the behaviour for $z \to \infty$. Their result can be formulated as follows:

THEOREM 4.1. *Let $y(z)$ be an arbitrary solution of Equation (53). Then the following assertions hold for $y(z)$:*

(a) $y(z)$ *is smooth for every* $z \in \mathbb{R}$ *and has the following asymptotic as* $z \to -\infty$*:*

$$y(z) = \gamma(-z)^{-1/4} \sin\left\{\frac{2}{3}\,(-z)^{3/2} + \frac{3}{4}\,\gamma^2 \ln(-z) + \xi_{10}\right\} + o((-z)^{-1/4}), \tag{55}$$

where the numbers $\gamma > 0$ *and* $0 \le \xi_{10} < 2\pi$ *may be arbitrary and are parameters of the solution* $y(z)$*.*

(b) If the parameters γ *and* ξ_{10} *of the solution* $y(z)$ *are connected by the relation*

$$\xi_{10} = \frac{3}{2}\,\gamma^2 \ln 2 - \frac{\pi}{4} - \arg\Gamma\left(i \cdot \frac{\gamma^2}{2}\right) + \delta\pi (\mathrm{mod}\, 2\pi), \qquad \delta = 0, 1, \tag{56}$$

then as $z \to +\infty$ *the solution* $y(z)$ *decreases exponentially:*

$$y(z) = \frac{a}{2\sqrt{\pi}}\, z^{-1/4} e^{-2z^{3/2}/3}(1 + o(1)), \tag{57}$$

where $a^2 = \exp(\pi\gamma^2) - 1$ *and* $\mathrm{sign}(a) = 2(1/2 - \delta)$*.*

(c) If (56) fails to hold (the general case), then as $z \to +\infty$ *the solution grows polynomially:*

$$y(z) = \pm\sqrt{z/2} \pm (2z)^{-1/4}\beta \cos\left\{\frac{2\sqrt{2}}{3}\, z^{3/2} - \frac{3}{2}\,\beta^2 \ln z + \xi_{20}\right\} + o(z^{-1/4}). \tag{58}$$

(d) In the asymptotics (58) all values of $\beta > 0$ *and* $0 \le \xi_{20} < 2\pi$ *are possible; these quantities characterize the solution* $y(z)$ *uniquely. The parameters* β*,* ξ_{20} *and the choice of the sign in (58) are uniquely determined from the parameters* γ *and* ξ_{10}

$$\beta^2 = \frac{1}{\pi}\, \ln \frac{1 + |p|^2}{2|\mathrm{Im}\, p|}\,, \tag{59a}$$

$$\xi_{20} = -\frac{3\pi}{4} - \frac{7}{2}\,\beta^2 \ln 2 + \arg\Gamma(i\beta^2) + \arg(1 + p^2), \tag{59b}$$

where

$$p = (\exp(\pi\gamma^2) - 1)^{1/2} \exp\left(i\frac{3}{2}\,\gamma^2 \ln 2 - i\frac{\pi}{4} - i \arg\left(\frac{i\gamma^2}{2}\right) - i\xi_{10}\right) \tag{59c}$$

and the upper sign in (58) is taken if $\mathrm{Im}\, p < 0$*.* □

We refer to [2] for a proof of this theorem and for the asymptotic description of the solution of the second Painlevé equation. This result confirms our asymptotic results and connects the integration constants in the asymptotic solution for $z \to -\infty$ with those in the one for $z \to +\infty$. Moreover, separating solutions, that follow the unstable branch beyond the bifurcation point, are singled out. We have now illustrated that the integration constants of the local solutions before, during and after crossing the supercritical bifurcation point can be connected. Because of symmetry reasons and since the map, as formulated in Theorem 4.1, is invertible, we can now construct a Poincaré map for one forcing period $2\pi/\varepsilon$ that connects the integration constants of a solution on a time t before crossing the supercritical bifurcation

point with those on a time $t+2\pi/\varepsilon$. The initial conditions of the original system (8) are chosen such that motions will be in a particular well after passage of the bifurcation point. From the analysis of Sections 3 and 4 it follows that motion outside the homoclinic loop separatrix does not occur after each passage of the bifurcation point on a time scale $O(1/\varepsilon)$.

5. The Construction of a Poincaré Map

In this section we construct a Poincaré map for one forcing period. With this map we can predict the complex dynamics of the system. The theorems on the composed asymptotic solutions prove the validity of these approximations on a time scale $O(1/\varepsilon)$, so the predictions are also valid on this time scale. In order to construct this Poincaré map we will consider four maps that connect the integration constants of the local asymptotic solutions valid at the begin-point and end-point of four different time intervals of $\tau = \varepsilon t$:

$$\text{I}: \qquad \tau \in \left[-\frac{\pi}{2} + 2\pi n - M\varepsilon^{2/3}, -\frac{\pi}{2} + 2\pi n + M\varepsilon^{2/3}\right], \qquad n \in \mathbb{Z}, \tag{60a}$$

$$\text{II}: \qquad \tau \in \left[-\frac{\pi}{2} + 2\pi n + M\varepsilon^{2/3}, \frac{\pi}{2} + 2\pi n - M\varepsilon^{2/3}\right], \tag{60b}$$

$$\text{III}: \qquad \tau \in \left[\frac{\pi}{2} + 2\pi n - M\varepsilon^{2/3}, \frac{\pi}{2} + 2\pi n + M\varepsilon^{2/3}\right], \tag{60c}$$

$$\text{IV}: \qquad \tau \in \left[\frac{\pi}{2} + 2\pi n + M\varepsilon^{2/3}, \frac{3\pi}{2} + 2\pi n - M\varepsilon^{2/3}\right], \tag{60d}$$

with M an arbitrary positive constant. In Section 4 it has been proven that the different local asymptotic solutions can be matched and the integration constants can be connected. Two parameters, the damping parameter k and the small parameter ε, have to be taken into account. The composition of the four different maps yields the Poincaré map. Regions I and III are the transition regions. Region II represents the outer region above the critical point, whereas region IV represents the outer region below the critical point. It has been shown in Section 4 that the matching conditions of (53) are given by (54a) and (54b) where γ, ξ_{10}, β and ξ_{20} are integration constants. With the aid of the results of Section 3 we obtain connection maps for the local integration constants. We take as initial values $\gamma = \gamma(0)$ and $\xi_{10} = \xi_{10}(0)$, and assume that this is a generic choice meaning that the separating condition (56) is not satisfied. In Figure 5 the construction of the Poincaré map is sketched.

Then the maps are as follows:

Region I:

$$f_1(\gamma(0), \xi_{10}(0)) \to (\beta(0), \xi_{20}(0), \sigma(0)), \tag{61a}$$

where

$$\beta^2(0) = \frac{1}{\pi}\ \ln\frac{1+|p|^2}{2|\text{Im}\ p|}\,, \tag{61b}$$

$$\xi_{20}(0) = -\frac{3\pi}{4} - \frac{7}{2}\ \beta^2(0)\ln 2 + \arg\Gamma(i\beta^2(0)) + \arg(1+p^2), \tag{61c}$$

$$\sigma(0) = -\text{sign}(\text{Im}\ p), \tag{61d}$$

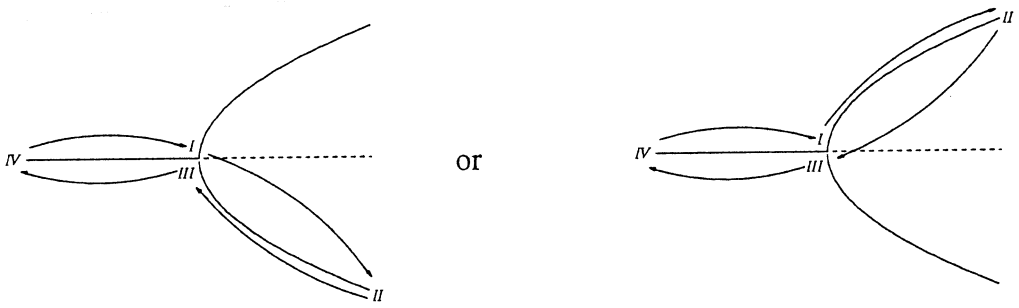

(5a) (5b)

Figure 5. With the aid of four time intervals the Poincaré map is constructed.

with

$$p = (e^{\pi\gamma^2(0)} - 1)^{1/2} \exp\left(i \cdot \frac{3}{2}\,\gamma^2(0) \ln 2 - i \cdot \frac{\pi}{4} - i \arg\Gamma\left(\frac{i\gamma^2(0)}{2}\right) - i\xi_{10}(0)\right). \quad (61e)$$

The sign of σ determines which branch will be approached after passage of the supercritical bifurcation point. If $\sigma = 1$ it will be the upper branch, while the lower branch will be followed for $\sigma = -1$. In the asymptotics both for $\sigma = 1$ and for $\sigma = -1$ all values of $\beta(0) > 0$ and $0 \le \xi_{20}(0) < 2\pi$ are possible.

Region II:

$$f_2(\beta(0), \xi_{20}(0)) \to (\beta_1(0), \xi_{21}(0)), \quad (62a)$$

where

$$\beta_1(0) = \beta(0) g_1(k), \quad (62b)$$

$$\xi_{21}(0) = -\frac{\sqrt{2}\,B(1/2, 3/4)}{\varepsilon} - \frac{3}{2}\,\beta^2(0) g_2(k) + g_3(k) - \xi_{20}(0), \quad (62c)$$

with

$$g_1(k) = \exp\left(\frac{-k\pi}{2}\right), \quad (62d)$$

$$g_2(k) = \ln\left(\frac{\varepsilon^{2/3}}{2}\right)(e^{-k\pi} + 1) - k\int_0^{\pi} \ln\left(\frac{1 - \cos s}{\sin s}\right) e^{-ks}\, \mathrm{d}s, \qquad g_3(k) = o(1). \quad (62e)$$

Region III:

$$f_3(\beta_1(0), \xi_{21}(0), \sigma(0)) \to (\gamma_1(0), \xi_{11}(0)), \quad (63a)$$

where

$$\gamma_1(0) = \left(\frac{\ln(1 + |p_1|^2)}{\pi}\right)^{1/2}, \quad (63b)$$

$$\xi_{11}(0) = \frac{3}{2}\,\gamma_1^2(0)\ln 2 - \frac{\pi}{4} - \arg\Gamma\left(\frac{i\gamma_1^2(0)}{2}\right) - \arg p_1, \tag{63c}$$

with

$$|p_1| = \left\{2\exp(2\pi\beta_1^2(0)) - 1 - 2\exp(\pi\beta_1^2(0))\sqrt{\exp(2\pi\beta_1^2(0)) - 1}\right.$$
$$\left.\times\ \cos\left(-\frac{3\pi}{4} - \frac{7}{2}\,\beta_1^2(0)\ln 2 + \arg\Gamma(i\beta_1^2(0)) + \xi_{21}(0)\right)\right\}^{1/2}, \tag{63d}$$

$$s = \text{sign}\left(\sin\left(-\frac{3\pi}{4} - \frac{7}{2}\,\beta_1^2(0)\ln 2 + \arg\Gamma(i\beta_1^2(0)) + \xi_{21}(0)\right)\right), \tag{63e}$$

$$\arg p_1 = \frac{1}{2}\,\pi(s\sigma(0)+1) - s\sigma(0)\arcsin\left(-\sigma(0)\frac{1+|p_1|^2}{2|p_1|\exp(\pi\beta_1^2(0))}\right). \tag{63f}$$

The map f_3 is the inverse map of f_1.

Region IV:

$$f_4(\gamma_1(0), \xi_{11}(0)) \to (\gamma(1), \xi_{10}(1)), \tag{64a}$$

where

$$\gamma(1) = \gamma_1(0)g_1(k), \tag{64b}$$

$$\xi_{10}(1) = \pi + \frac{3}{4}\,\gamma_1^2(0)g_2(k) - \frac{B(1/2,3/4)}{\varepsilon} + \sqrt{2}\,g_3(k) - \xi_{11}(0), \tag{64c}$$

with $g_1(k)$, $g_2(k)$ and $g_3(k)$ as defined in (62d) and (62e).

We have now obtained a Poincaré map for one forcing period

$$P(\gamma(0), \xi_{10}(0)) := f_4 \circ f_3 \circ f_2 \circ f_1(\gamma(0), \xi_{10}(0)) = (\gamma(1), \xi_{10}(1)). \tag{65}$$

This is a two-dimensional map that contains the parameters k and ε. With the aid of this map the complex dynamics of system (8) can be analyzed. Depending on the initial conditions and the values of the parameters it is possible to predict which stable branch will be followed after crossing the supercritical bifurcation point in the course of each forcing period. In the next section the dynamics of the Poincaré map (65) are considered.

REMARK. It is possible to consider the Poincaré map for different values of the parameter k as an order function in ε. Let

$$k = \kappa\varepsilon^{\alpha}, \qquad \alpha \geq -\frac{1}{2}\,, \tag{66}$$

then $g_1(k) = \exp(-k\varepsilon^{\alpha}/2)$ and for the functions $g_2(k)$ and $g_3(k)$, defined in (62e), we obtain

$$\alpha = -\frac{1}{2}\ :\quad g_2(k) = \ln(\kappa\varepsilon^{1/6}) + \gamma + o(1), \qquad g_3(k) = \frac{\kappa^2 K(1/2)}{4}\,, \tag{67a}$$

$$-\frac{1}{2} < \alpha < 0: \quad g_2(k) = \ln(\kappa\varepsilon^{(2/3)+\alpha}) + \gamma + o(1), \qquad g_3(k) = o(1), \tag{67b}$$

$$\alpha = 0: \quad g_2(k) = \ln\left(\frac{\varepsilon^{2/3}}{2}\right)(e^{-\kappa\pi}+1) - \kappa\int_0^{\pi} \ln\left(\frac{1-\cos s}{\sin s}\right) e^{-\kappa s}\,\mathrm{d}s + o(1),$$

$$g_3(k) = o(1), \tag{67c}$$

$$\alpha > 0: \quad g_2(k) = 2\ln\left(\frac{\varepsilon^{2/3}}{2}\right) + o(1), \qquad g_3(k) = o(1). \tag{67d}$$

6. Analysis of the Poincaré Map

The Poincaré map, that has been constructed in Section 5, has the following form for m forcing periods, $m \in \mathbb{N}$,

$$P^m(\gamma(0), \xi_{10}(0)) = (\gamma(m), \xi_{10}(m)). \tag{68}$$

It follows that

$$(\beta(m), \xi_{20}(m), \sigma(m)) = f_1(\gamma(m), \xi_{10}(m)), \tag{69}$$

with f_1 as defined in (61). The complex dynamics of system (8) may be characterized by monitoring the position of a motion once per forcing cycle. With the aid of the Poincaré map it can be predicted on a time scale $O(1/\varepsilon)$ which stable branch, the upper (U) or the lower (L), will be followed after crossing the bifurcation point $\cos(\varepsilon t) = 0$ from below after each forcing cycle. This is determined by the sign of $\sigma(m)$. This $\sigma(m)$, $m \geq 0$, is defined in (69). In this way we obtain a symbol sequence of U's ($\sigma(m) = 1$) and L's ($\sigma(m) = -1$). Moreover, Lyapunov exponents of the two-dimensional Poincaré map can be computed. These exponents describe the structure of the attractor of the orbits. The system exhibits a strange attractor if one of these exponents is positive. The conjecture of Kaplan and Yorke provides the value of the fractal dimension of this attractor. The Poincaré map can exhibit sensitive dependence on initial conditions, a criterion for chaos.

We now introduce the following definitions

$$x_i = (\gamma(i-1), \xi_{10}(i-1))', \qquad x_{i+1} = P(x_1) \quad (P \text{ as defined in (65)}), \tag{70a}$$

$$M(x) = \frac{\partial P}{\partial x}(x) \quad \text{(the Jacobian of } P\text{)}. \tag{70b}$$

We define the two (possibly complex) eigenvalues $\lambda_1(n)$, $\lambda_2(n)$ with $|\lambda_1(n)| \geq |\lambda_2(n)|$ of the matrix

$$A_n = [M(x_n)M(x_{n-1})\ldots M(x_1)]^{1/n}. \tag{71}$$

The Lyapunov exponents are then given by

$$v_j(x_1) = \lim_{n\to\infty} \ln|\lambda_j(n)|, \qquad j = 1, 2. \tag{72}$$

Another way to obtain these Lyapunov exponents is by introducing the eigenvalues λ_{1i}, λ_{2i} of the M matrix $M(x_i)$ with $|\lambda_{1i}| \geq |\lambda_{2i}|$, from which we obtain the Lyapunov exponents

$$v_j(x_1) = \lim_{n\to\infty} \frac{1}{n} \sum_{i=1}^{n} \ln|\lambda_{ji}|, \qquad j = 1, 2. \tag{73}$$

Roughly speaking, the Lyapunov exponents of a given trajectory characterize the mean exponential rate of divergence of trajectories surrounding it. The mean exponential rate of growth of the phase space area is defined by

$$v(x_1) = v_1(x_1) + v_2(x_1). \tag{74}$$

For a measure-preserving flow, of which system (8) without damping is a special case, we see that

$$v_1(x_1) + v_2(x_1) = 0, \tag{75}$$

while for a dissipative system (system (8) with the damping parameter k not equal to zero) this sum must be negative. Note that for the starting point x_1 of an orbit arbitrarily chosen, the Lyapunov exponents can be different when the parameters are fixed. Their sum, however, is a fixed value in that case. We now first consider system (8) without damping ($k = 0$) and, next, we examine the dissipative case ($k \neq 0$).

6.1. The Non-Dissipative Case

In the case without damping Equation (8) describes the dynamics of a slowly varying Hamiltonian system. Due to the absence of damping Hamiltonian chaos will occur, see, e.g. [3]. The Poincaré map is area-preserving and, therefore, there are two possibilities for the Lyapunov exponents of this map:

$$\text{I}: \qquad v_1(x_1) > 0 > v_2(x_1) = -v_1(x_1), \tag{76a}$$

$$\text{II}: \qquad v_1(x_1) = v_2(x_1) = 0. \tag{76b}$$

In the first case the orbits are chaotic and there exists a chaotic attractor of dimension 2. In the second case the KAM-theorem (see, e.g., Ott [18]) provides an answer to the question in which way orbits will behave: with probability 1 the attractor is quasiperiodic of dimension 1. For fixed values of the parameters the Poincaré map exhibits both order and chaos depending on the initial state of an evolution. We observe quasiperiodic orbits with closed curves belonging to them and chaotic orbits; it is a matter of "order in a sea of chaos".

We illustrate the situation with the help of some figures. In Figure 6 the Lyapunov exponents are shown for a certain (fixed) initial state for different values of ε. As can be seen from this figure the sum of the Lyapunov exponents is equal to zero. From this figure it can be concluded that the system exhibits a quasiperiodic orbit for the initial state $\xi_{10}(0) = \pi$, $\gamma(0) = 1.875$ when $\varepsilon = 0.3$. In Figure 7 it is shown that for $\varepsilon = 0.3$ the phase portrait of $(\gamma \sin\xi_{10}, \gamma\cos\xi_{10})$ exhibits besides chaotic orbits also quasiperiodic orbits that form dense closed curves. Moreover, it is illustrated that the modulus of the eigenvalues of A_n (see (71)) tends to one when the number of iterations is enlarged in the quasiperiodic case. In the chaotic case the modulus of the largest eigenvalue will always remain larger than one.

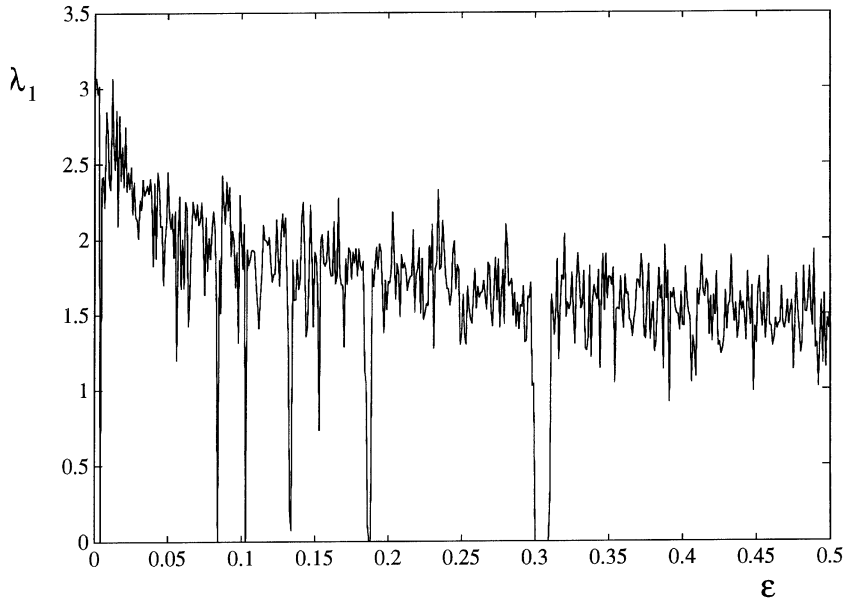

(a)

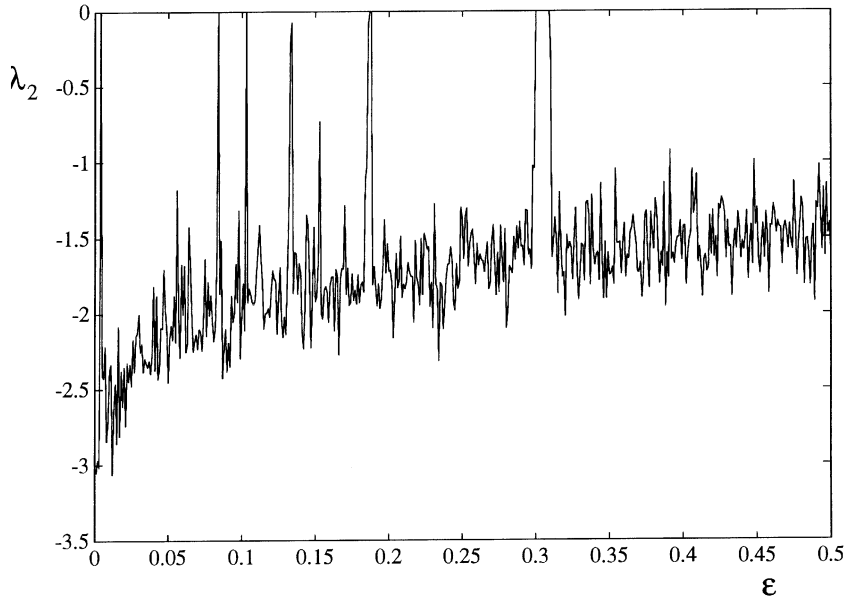

(b)

Figure 6. The first (a) and second (b) Lyapunov exponent for the Poincaré map in the non-dissipative case. The (fixed) initial state is $x_1 = (\gamma(0), \xi_{10}(0))^t = (1.875, \pi)^t$.

6.2. THE CASE WITH DAMPING

When the damping parameter k in Equation (8) is strictly positive the system is dissipative. This means for the sum of the Lyapunov exponents for the Poincaré map:

$$v_1(x_1) + v_2(x_2) < 0, \tag{77}$$

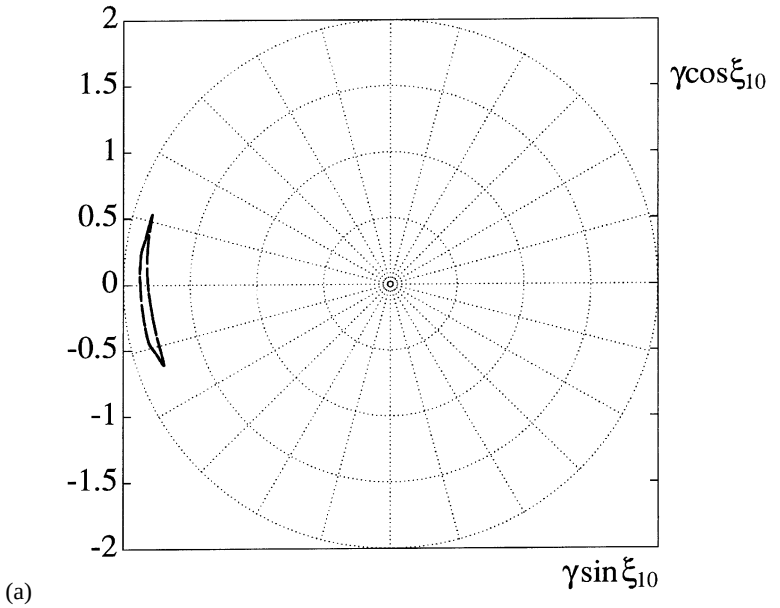

(a)

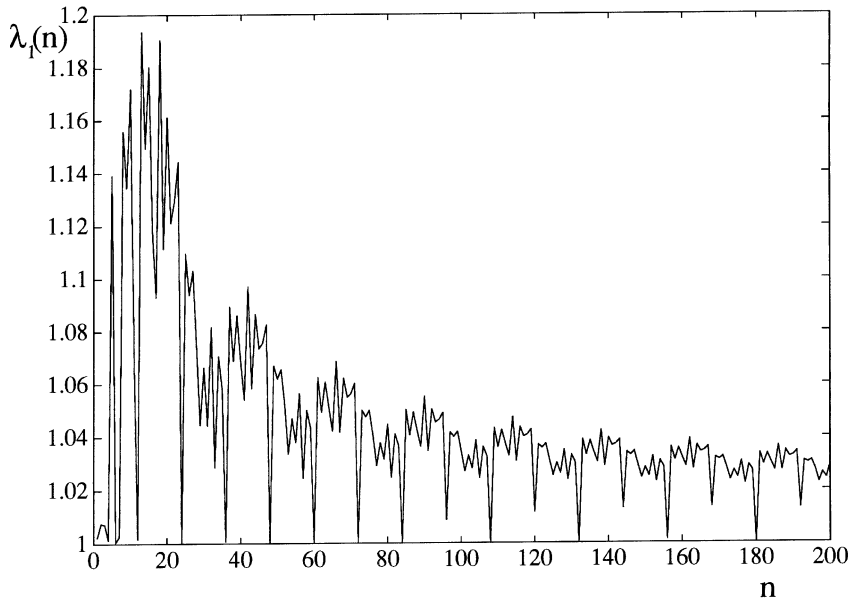

(b)

Figure 7. For $\varepsilon = 0.3$ both a quasiperiodic orbit (a) with $x_1 = (1.875, \pi)^t$ and a chaotic orbit (c) with $x_1 = (1.875, \pi/2)^t$ are possible. The modulus of the largest eigenvalue of the matrix A_n tends to one for $x_1 = (1.875, \pi)^t$ (b) and for $x_1 = (1.875, \pi/2)^t$ it remains larger than one. The phase portrait (e) of $(\gamma \sin\xi_{10}, \gamma \cos\xi_{10})$ shows that the Poincaré map exhibits quasiperiodic orbits and chaotic orbits.

so the volume (area) in phase space decreases under the mapping. Similar to the frictionless case we can distinguish two possibilities:

$$\text{I}: \quad 0 \geq v_1(x_1) \geq v_2(x_1), \quad v_1(x_1) \neq v_2(x_1) \quad \text{if} \quad v_1(x_1) = 0, \tag{78a}$$

$$\text{II}: \quad v_1(x_1) > 0 > v_2(x_1). \tag{78b}$$

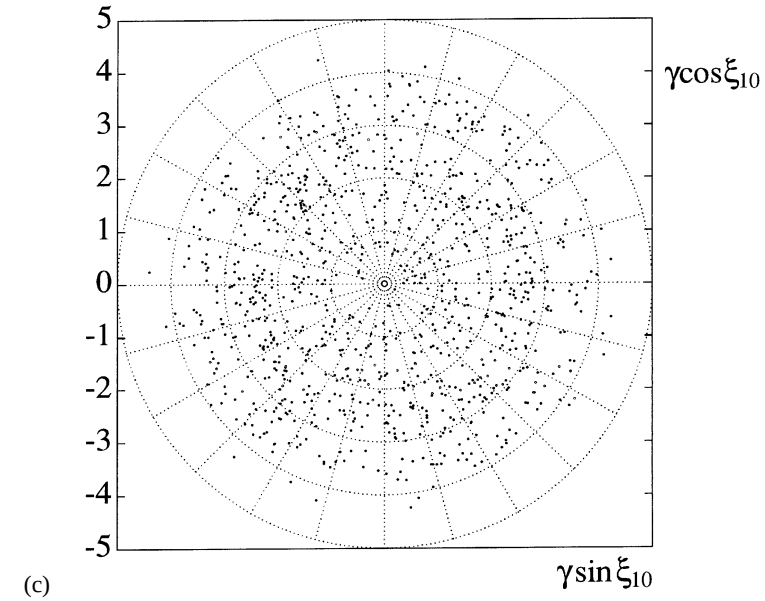

(c)

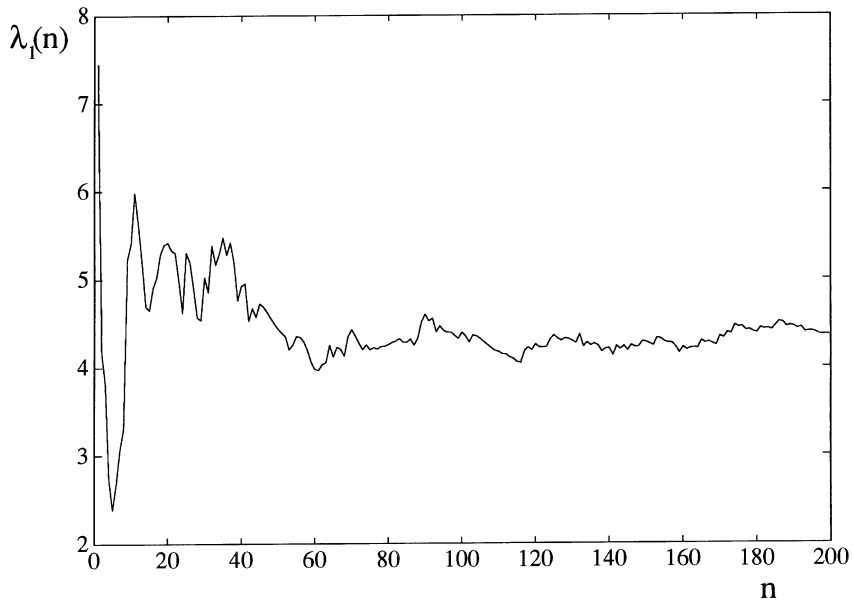

(d)

Figure 7. (Continued)

In the first case the system possesses a periodic attractor. In the second case the attractor is chaotic. Following Lichtenberg and Lieberman [3] we compute the fractal dimension d of this chaotic attractor with the aid of the conjecture of Kaplan and Yorke:

$$d = 1 - \frac{v_1(x_1)}{v_2(x_1)} \,. \tag{79}$$

The situation is again illustrated with the aid of some figures. In all figures illustrating the dissipative case the parameter ε is chosen $\varepsilon = 0.1$. The Lyapunov exponents for a certain

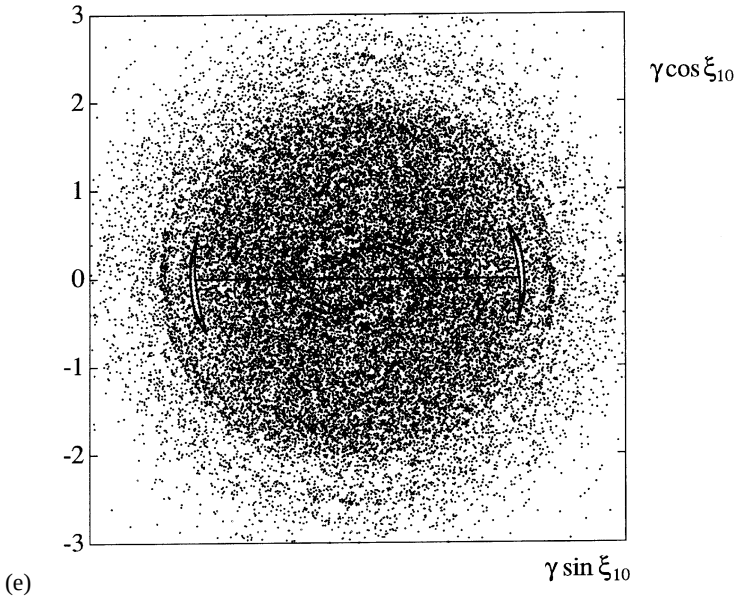

(e)

Figure 7. (Continued)

(fixed) initial state for different values of k are depicted in Figure 8. The values that the state variables of the Poincaré map will take after a certain number of iterations for different values of k, are shown in Figure 9. In Figure 10 it is seen that the rate at which the volume in phase space decreases, becomes smaller when k decreases and ε is fixed. Due to the damping, that is of order $O(k\varepsilon)$, and the forcing period, that is equal to $2\pi/\varepsilon$, we obtain for the phase space volume (area) decreasing rate:

$$v_1(x_1) + v_2(x_2) = O(-2k\pi). \tag{80}$$

This rate is only dependent on the value of the parameter k, so it does not depend on the initial state of the system. In Figure 11 the dimension of the attractor of orbits with a certain initial state is computed as a function of k. Finally, in Figure 12, it is shown that for $k = 0.05$ and $\varepsilon = 0.1$ the system exhibits a chaotic attractor. The fractal dimension of this attractor – obtained with the aid of the conjecture of Kaplan and Yorke – is 1.8623.

REMARK. When $k = \kappa\varepsilon^{\alpha}$, $\alpha \geq -0.5$, the phase space volume (area) decreasing rate does also depend on ε:

$$v_1(x_1) + v_2(x_2) = O(-k\pi\varepsilon^{\alpha}). \tag{81}$$

REMARK. The computation of the Jacobian M of the Poincaré map requires a considerable amount of analytical calculations as well as computing time necessary for the evaluation of the Lyapunov exponents from the product of Jacobians of a sufficiently large number of points of an orbit. For the computation of the Jacobian we refer to the Appendix.

7. A Comparison between the Analytical Results and Numerical Simulations

In this section we compare results of numerical simulations with the analytical approximations derived in the foregoing sections. The simulations have been carried out for the

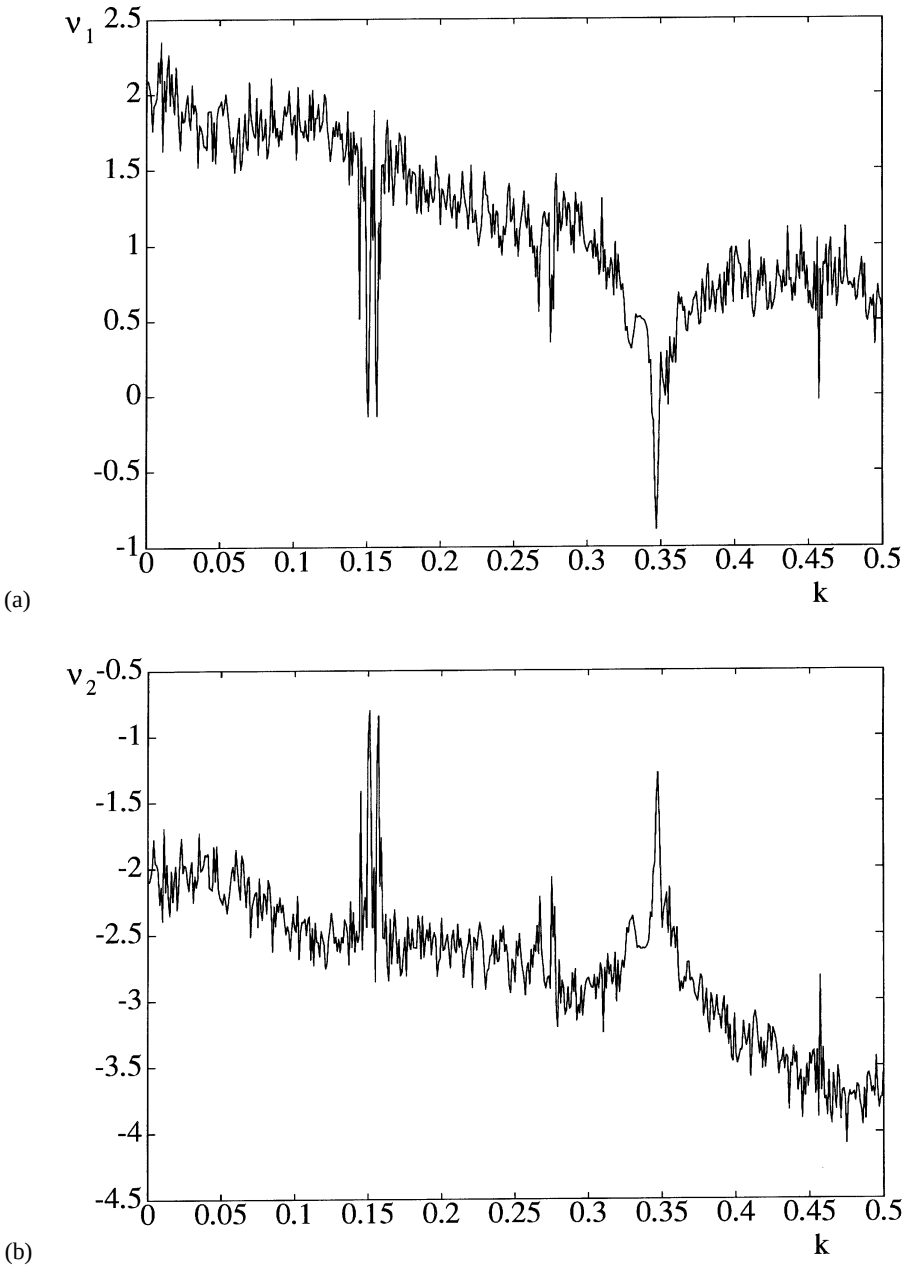

Figure 8. The first ($v_1(x_1)$) and second ($v_2(x_1)$) Lyapunov exponents for the Poincaré map in the dissipative case with $\varepsilon = 0.1$. The fixed initial state is $x_1 = (1.875, \pi)^t$.

system described in Equation (8) by following the path of the state (x, x') for initial states $(x(t_0), x'(t_0))$. We assume for the initial forcing $G(t_0) = -1$. We consider both the conservative and the dissipative case. In order to compare the results we take a Poincaré section when the forcing term $G(t) = -1$. The Poincaré map constructed in Section 5 needs a little adjustment. The analytical way in which we obtained this map, however, does not change. The integration constants of the solution at time points where $G(t) = -1$ yield a value for the

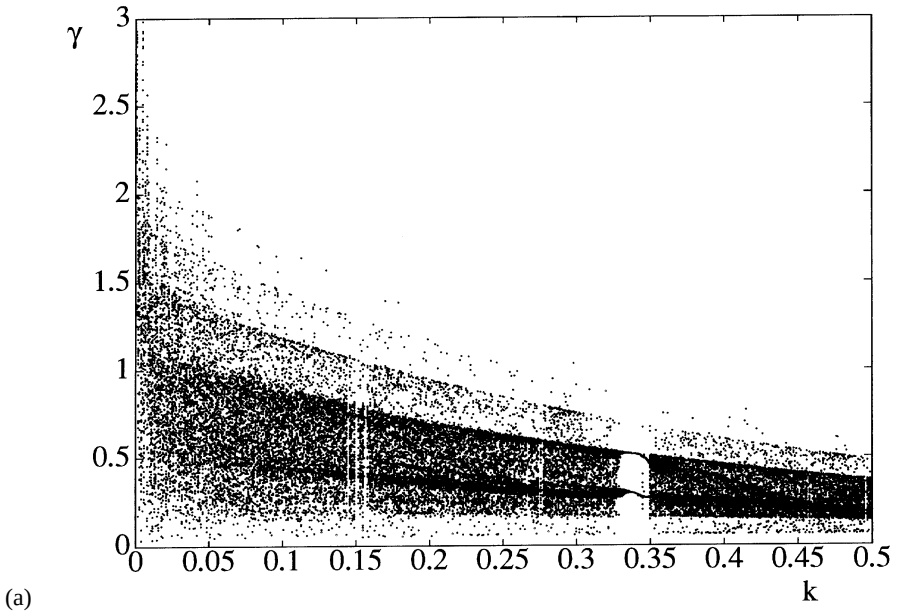

(a)

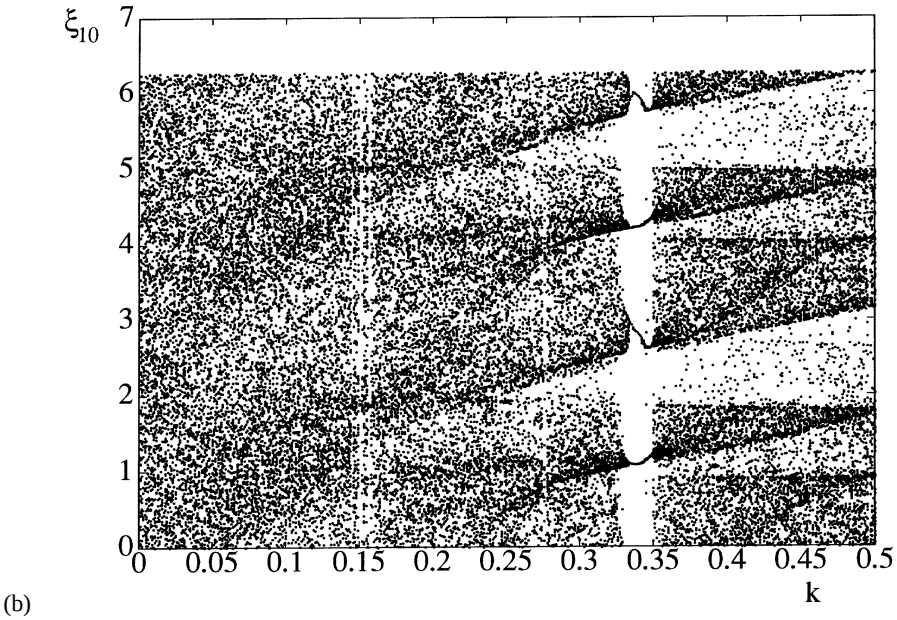

(b)

Figure 9. The limit values that the state variables of the mapping, γ and ξ_{10}, will take for different values of k when $\varepsilon = 0.1$ and $x_1 = (1.875, \pi)^t$.

parameter σ that determines which stable branch will be followed after crossing the bifurcation point. In Table 1 we give results for one of the integration constants after some periods when $G(t) = -1$. Furthermore, it is described with the aid of the parameter σ which branch will be followed after the next crossing of the bifurcation point $G(t) = 0$ from below.

The analytical approximations are in reasonably good accordance with the numerical simulation results after a small number of forcing periods. However, when the number of

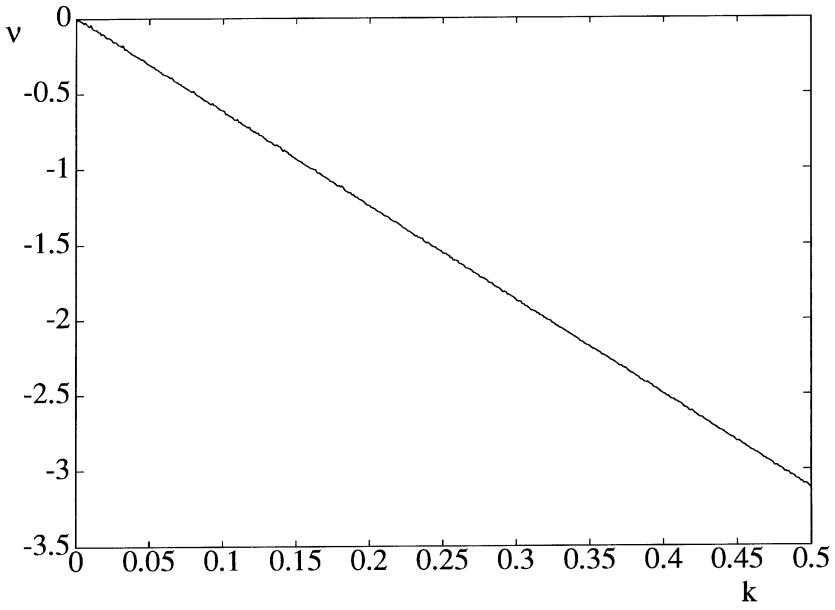

Figure 10. The rate $v_1(x_1) + v_2(x_1)$ at which the phase space area decreases for $\varepsilon = 0.1$ when k is varied. This rate is independent of the initial state x_1.

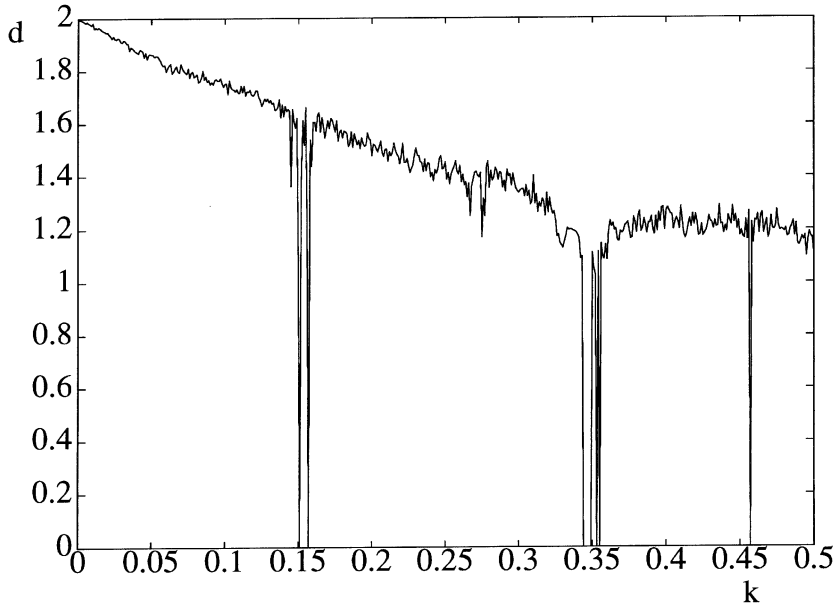

Figure 11. The (fractal) dimension of the attractor for $\varepsilon = 0.1$ and $x_1 = (1.875, \pi)^t$ for different values of ε. This dimension is obtained with the aid of the conjecture of Kaplan and Yorke. Note that there is indeed a chaotic attractor when the first Lyapunov exponent is larger than zero. (Compare this figure with Figure 8a.)

forcing periods is increased, the approximations can deviate enormously. For the initial state that is chosen in Table 1a, the analytical and numerical approximations yield a quasiperiodic solution. When a periodic attractor arises in the dissipative case for both approximations there

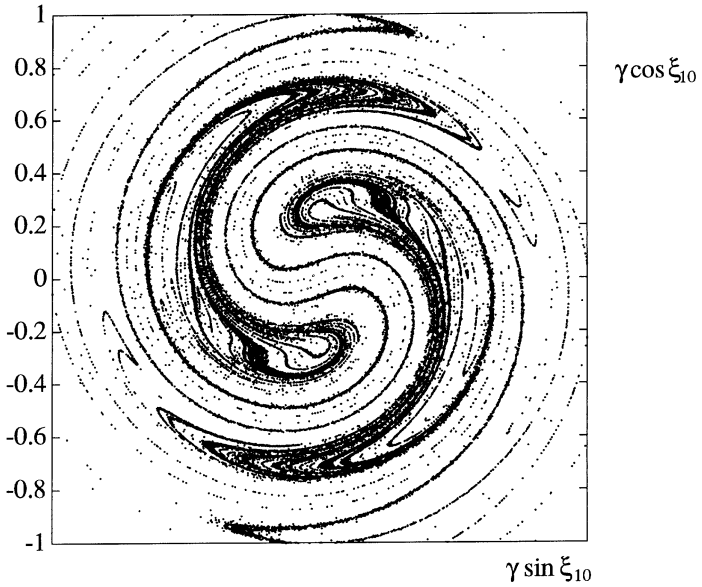

Figure 12. For $k = 0.05$ and $\varepsilon = 0.1$ for $x_1 = (1.875, \pi)^t$ chaos appears in the Poincaré map. The phase portrait of $(\gamma \sin\xi_{10}, \gamma \cos\xi_{10})$ is illustrated.

Table 1. The integration constants $x(t_0 + 2\pi i/\varepsilon)$ and $x'(t_0 + 2\pi i/\varepsilon)$ of the solutions after i forcing periods. Moreover, it is indicated with $\sigma(i)$ which stable branch (U = Upper, L = Lower) will be followed after crossing the bifurcation point from below $i + 1$ times. The subscripts n and a denote respectively numerical and analytical approximations.

(a) $k = 0$, $\varepsilon = 0.004$, $(x(t_0), x'(t_0), G(t_0)) = (0, -0.1184, -1)$					
	$x_a(t_0 + i\frac{2\pi}{\varepsilon})$	$x'_a(t_0 + i\frac{2\pi}{\varepsilon})$	$x_n(t_0 + i\frac{2\pi}{\varepsilon})$	$x'_n(t_0 + i\frac{2\pi}{\varepsilon})$	$\sigma(i)$
$i = 0$	0.0000	−0.1184	0.0000	−0.1184	−1(L)
$i = 1$	−0.0026	0.1185	−0.0107	0.1186	1(U)
$i = 2$	0.0011	−0.1186	0.0028	−0.1195	−1(L)
$i = 3$	0.0022	0.1186	0.0141	0.1187	1(U)
$i = 4$	−0.0019	−0.1184	−0.0208	−0.1174	−1(L)
$i = 5$	−0.0014	0.1184	0.0112	0.1181	1(U)
(b) $k = 1.25$, $\varepsilon = 0.1$, $(x(t_0), x'(t_0), G(t_0)) = (0.04, 0, -1)$					
$i = 0$	0.0400	0.0000	0.0400	0.0000	1(U)
$i = 1$	0.0398	−0.0427	0.0465	−0.0454	1(U)
$i = 2$	0.0429	−0.0488	0.0480	−0.0457	1(U)
$i = 3$	0.0433	−0.0490	0.0472	−0.0456	1(U)
$i = 4$	0.0432	−0.0490	0.0476	−0.0456	1(U)
$i = 5$	0.0432	−0.0490	0.0474	−0.0456	1(U)

is a good agreement between the numerical and analytical resultss even for $t \to \infty$. This is the case for the initial chosen in Table 1b. The parameter k is deliberately chosen somewhat larger than in previous discussions, so that it can be seen that a periodic attractor arises in this case. When the approximations yield chaotic solutions, they will deviate after a few number

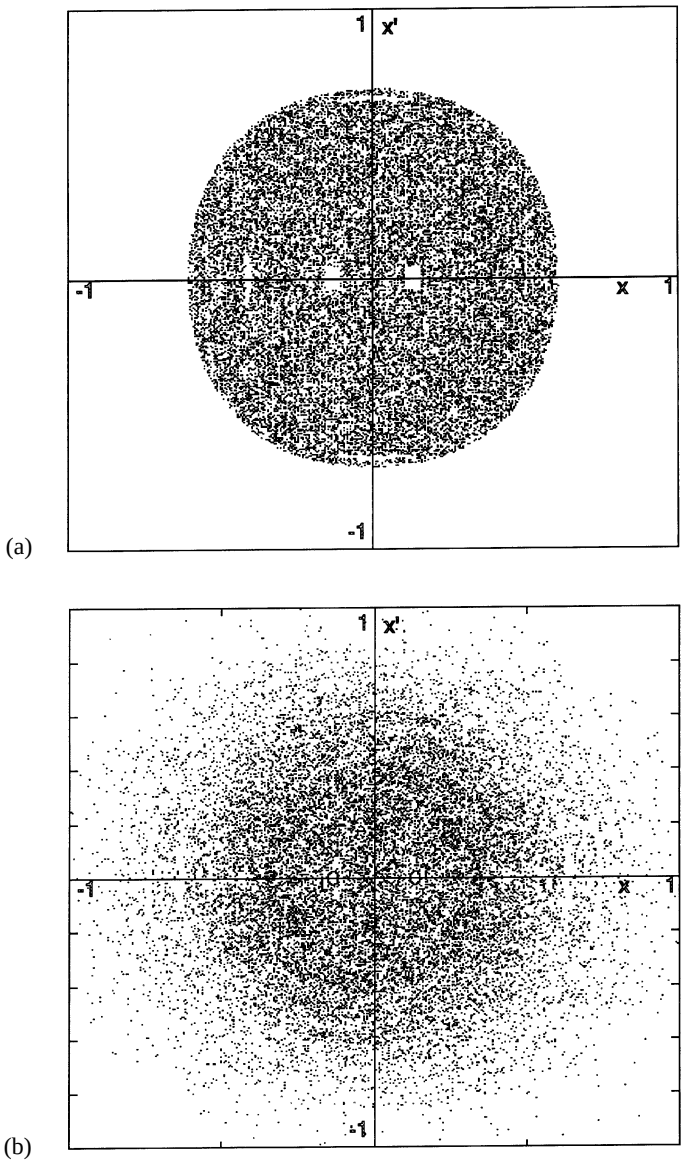

Figure 13. Poincaré map of the x–x' plane for one forcing period of Equation (8) with $k = 0$ and $\varepsilon = 0.084$. The maps are obtained by numerical integration of Equation (8) (a) and by numerical calculations for the analytical expressions (b). Note the familiar KAM-patterns of islands of order in a sea of chaos.

of iterations due to the sensitive dependence on computational errors and on initial conditions. Differences between the numerical and analytical results can be due to omitting higher order terms in the calculations of the analytical expressions, to numerical computational errors, and to the sensitive dependence on initial conditions. When ε becomes smaller, the analytically obtained asymptotic solution will yield a better approximation.

In Figures 13 and 14 we compare the numerically obtained Poincaré surface of section of the intersection of trajectories $(x(t), x'(t))$ with the surface of section $t = t_0 + 2n\pi/\varepsilon$, $n \in \mathbb{Z}$, with the Poincaré map obtained by analytical methods in the foregoing sections.

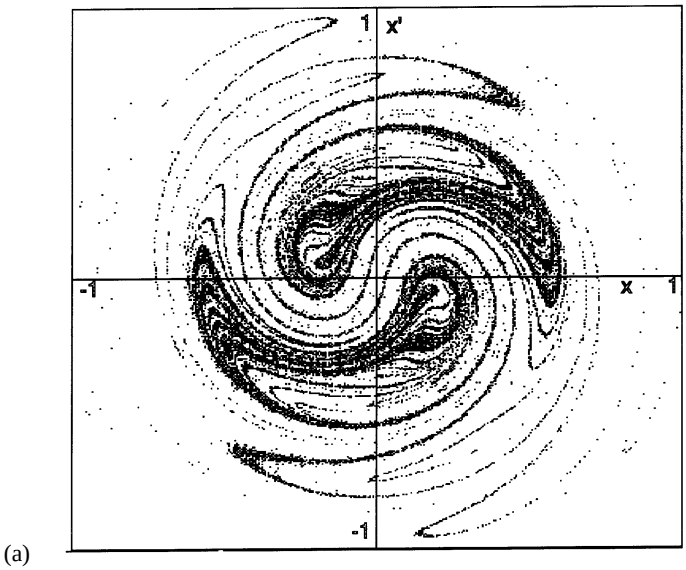

(a)

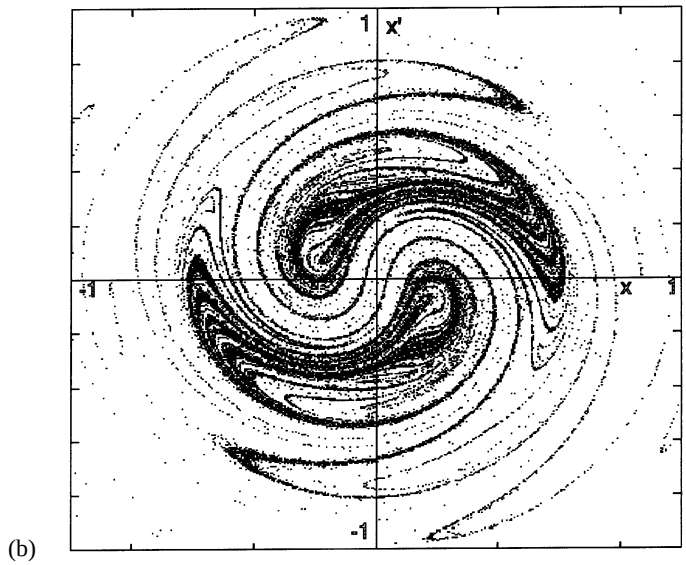

(b)

Figure 14. Poincaré map of the x–x' plane for one forcing period of Equation (8) with $k = 0.1$ and $\varepsilon = 0.1$. Again the result of numerical simulations (a) is compared with the map obtained by using analytical methods (b).

At first sight there does not seem to be a good agreement between the numerical and analytical results in the case without damping. However, Figure 13 illustrates the behaviour of solutions of Equation (8) for $t \to \infty$. For a certain number of iterations of the Poincaré map the analytical results correspond with the numerical results. Chaotic effects and numerical computational errors cause differences between the approximations that become larger when time increases. Both approximations, however, yield a similar structure of quasiperiodic orbits (e.g. if $(x(0), x'(0), G(0)) = (0.15, 0, -1)$ a quasiperiodic attractor appears in both cases).

Although ε is not chosen very small, the analytic approximation seems to be in accordance with the numerical simulation results in the dissipative case of Figure 14. The structure of

the attractor is very similar for both approximations. The sequence of stable branches, which will be followed after passage of the bifurcation point, however, is different for the two approximations.

In Bridge and Rand [4] the complex dynamical behaviour in the class of systems, of which the problem of this study is a prototype, has been identified as coming from several sources: effects of stretching along the unstable manifold of the saddle for a forcing above the critical value, quasiperiodic rotation, separatrix crossing, and Hamiltonian chaos. Consequently, by analyzing the Poincaré map for one forcing period, the results are only satisfactory for a certain number of iterations of the mapping. When ε is small the effect of omitting higher order terms in the calculations of the analytical expressions is not felt. For ε large, however, these higher order terms will produce a large effect, which also explains the difference between the approximations. In many cases, however, we can gain a better insight in the structure of the attractor of the Poincaré map, when using the analytical results.

8. Conclusion

In this paper we have analyzed a second order system with a slowly varying parameter. We considered the case of repeated passage of a pitchfork bifurcation. By using perturbation techniques the solution of the problem is approximated asymptotically. In order to obtain local asymptotic expansions both averaging and boundary layer methods turned out to be necessary. The dynamics on the large time scale where the solution oscillates around a (slowly varying) stable equilibrium solution is described with the aid of averaging methods. The approximation of the local outer solution above the bifurcation point requires "second order averaging", whereas "first order averaging" is sufficient to approximate the local outer solution below the bifurcation point. The validity of the asymptotic expansions is investigated and it is proven that the different local solutions overlap. The required information on the matching of the different locally valid asymptotic approximations is produced by an analytical study of the transition layer equation, which is the second Painlevé transcendent. There is a bijective connection between the integration constants of the slowly oscillating solutions that are valid before and after passage of the bifurcation point. Using the results of averaging methods, matching techniques and local connection formulas we can construct a Poincaré map for one forcing period that approximates the dynamics of the system.

The characteristics of the two-dimensional Poincaré map are analyzed by considering Lyapunov exponents and using the KAM-theorem in order to draw conclusions about the evolution of orbits. In the non-dissipative case for each value of the parameter there may be sensitive dependence on initial conditions, a criterion for chaos. This result confirms the results of Bridge and Rand [4] and of Coppola and Rand [6]. Both in the non-dissipative and in the dissipative case for fixed values of the parameters (quasi) periodic orbits, corresponding to closed curves in the phase portrait, and chaotic orbits are possible. With the aid of the Poincaré map the behaviour of the system can be predicted on a time scale $O(1/\varepsilon)$ given the initial state and the values of the parameters. It is possible to construct symbol sequences of U's (Upper branch) and L's (Lower branch) of the branch that will be followed after each crossing of the bifurcation point from below. The periodic bifurcation takes place on a relatively small time scale of length $\varepsilon t = O(\varepsilon^{2/3})$.

It is noted that there is a good correspondence between the results obtained by numerical simulation of the system and the analytical results based on the Poincaré map. After a large number of forcing periods, however, this agreement may disappear due to sensitive depen-

dence, numerical computational errors and the omission of higher order terms in calculating the analytical expressions. The analytical methods that are used in this study, are applicable to a wide class of (mechanical) problems for which the transition layer equation around the bifurcation points is described by the same second Painlevé transcendent. Consequently, the asymptotic matching conditions will have the same form as the conditions we have obtained in this study.

Acknowledgements

The author would like to thank Arjen Doelman for bringing to his attention the problem of this paper, and Johan Grasman for the discussions concerning the subject treated in this paper and for his remarks on the text.

Appendix: The Computation of the Poincaré Map

In this appendix we give the details of the computation of the Jacobian of the Poincaré map constructed in this study. We use the same notations as in Sections 5 and 6. Furthermore, we define

$$p = |p|e^{i\xi}, \qquad p_1 = |p_1|e^{i\xi_1}. \tag{A1}$$

In order to obtain the Jacobian we use the following results

$$\arg\Gamma(1+iy) = \arg\Gamma(iy) + \frac{1}{2}\,\pi, \qquad y > 0, \tag{A2}$$

$$\arg\Gamma(iy) = \mathrm{Im}(\ln\Gamma(iy)), \tag{A3}$$

$$\frac{\mathrm{d}}{\mathrm{d}y}\,\mathrm{Im}\left(\ln\Gamma\left(1+\frac{iy^2}{2}\right)\right) = y\mathrm{Re}\;\psi\left(1+\frac{iy^2}{2}\right), \tag{A4}$$

with $\psi(z)$ the Psi (Digamma) function. These results can be derived from the expressions 6.1.28, 6.1.44 and 6.3.1 in Abramowitz and Stegun [16]. It is now possible to compute partial derivatives for the transformations that have been carried out to construct a Poincaré map:

$$\begin{pmatrix} \dfrac{\partial|p|(j)}{\partial\gamma(j)} & \dfrac{\partial|p|(j)}{\partial\xi_{10}(j)} \\[2ex] \dfrac{\partial\xi(j)}{\partial\gamma(j)} & \dfrac{\partial\xi(j)}{\partial\xi_{10}(j)} \end{pmatrix} = \begin{pmatrix} \pi\gamma(j)e^{\pi\gamma^2(j)}(e^{\pi\gamma^2(j)}-1)^{-1/2} & 0 \\[2ex] 3\gamma(j)\ln 2 - \gamma(j)\mathrm{Re}\;\psi\left(1+\dfrac{i\gamma^2(j)}{2}\right) & -1 \end{pmatrix}, \tag{A5}$$

$$\begin{pmatrix} \dfrac{\partial\beta(j)}{\partial\gamma(j)} & \dfrac{\partial\beta(j)}{\partial\xi_{10}(j)} \\[2ex] \dfrac{\partial\xi_{20}(j)}{\partial\gamma(j)} & \dfrac{\partial\xi_{20}(j)}{\partial\xi_{10}(j)} \end{pmatrix} \tag{A6}$$

with

$$\frac{\partial\beta(j)}{\partial\gamma(j)} = \frac{\gamma(j)}{2\beta(j)}\left(\frac{e^{\pi\gamma^2(j)}-2}{e^{\pi\gamma^2(j)}-1} - \frac{3\ln 2 - \mathrm{Re}\;\psi(1+\frac{i\gamma^2(j)}{2})}{\pi\tan\xi(j)}\right),$$

$$\frac{\partial \xi_{20}(j)}{\partial \gamma(j)} = -B(j)\frac{\partial \beta(j)}{\partial \gamma(j)}\,(7\ln 2 - 2\mathrm{Re}\;\psi(1+i\beta^2(j))) + \frac{2|p|(j)(\frac{\partial |p|(j)}{\partial \gamma(j)}\,\sin 2\xi(j) + |p|(j)\frac{\partial \xi(j)}{\partial \gamma(j)}\,(\cos 2\xi(j) + |p|^2(j))}{1+|p|^2(j)(2\cos 2\xi(j)+|p|^2(j))}\,,$$

$$\frac{\partial \beta(j)}{\partial \xi_{10}(j)} = \frac{1}{2\pi\beta(j)\tan\xi(j)}\,,$$

$$\frac{\partial \xi_{20}(j)}{\partial \xi_{10}(j)} = \frac{-(7/2)\ln 2 + \mathrm{Re}\;\psi(1+i\beta^2(j))}{\pi\tan\xi(j)} - \frac{2|p|^2(j)(\cos 2\xi(j)+|p|^2(j))}{1+|p|^2(j)(2\cos 2\xi(j)+|p|^2(j))}\,,$$

$$\begin{pmatrix} \frac{\partial \beta_1(j)}{\partial \gamma(j)} & \frac{\partial \beta_1(j)}{\partial \xi_{10}(j)} \\ \frac{\partial \xi_{21}(j)}{\partial \gamma(j)} & \frac{\partial \xi_{21}(j)}{\partial \xi_{10}(j)} \end{pmatrix} \tag{A7}$$

with

$$\frac{\partial \beta_1(j)}{\partial \gamma(j)} = e^{-k\pi/2}\frac{\partial \beta(j)}{\partial \gamma(j)}\,,$$

$$\frac{\partial \xi_{21}(j)}{\partial \gamma(j)} = -3\beta(j)g_2(k)\frac{\partial \beta(j)}{\partial \gamma(j)} - \frac{\partial \xi_{20}(j)}{\partial \gamma(j)}\,,$$

$$\frac{\partial \beta_1(j)}{\partial \xi_{10}(j)} = \frac{e^{-k\pi/2}}{2\pi r\tan\xi(j)}\,,$$

$$\frac{\partial \xi_{21}(j)}{\partial \xi_{10}(j)} = -3\beta(j)g_2(k)\frac{\partial \beta(j)}{\partial \xi_{10}(j)} - \frac{\partial \xi_{20}(j)}{\partial \xi_{10}(j)}\,,$$

$$\begin{pmatrix} \frac{\partial |p_1|^2(j)}{\partial \beta_1(j)} \\ \frac{\partial |p_1|^2(j)}{\partial \xi_{21}(j)} \end{pmatrix} = \begin{pmatrix} \beta_1(j)e^{\pi\beta_1^2(j)}(8\pi e^{\pi\beta_1^2(j)} - 4\pi(e^{2\pi\beta_1^2(j)}-1)^{1/2}\cos(d) \\ \qquad -4\pi e^{2\pi\beta_1^2(j)}-1)^{-1/2}\cos(d)) \\ \qquad +2(e^{2\pi\beta_1^2(j)}-1)^{1/2}\sin(d)(7\ln 2 - 2\mathrm{Re}\;\psi(1+i\beta_1^2(j))) \\ 2e^{\pi\beta_1^2(j)}(e^{2\pi\beta_1^2(j)}-1)^{1/2}\sin(d) \end{pmatrix}, \tag{A8}$$

with

$$d = -\frac{3\pi}{4} - \frac{7}{2}\,\beta_1^2(j)\ln 2 + \arg\Gamma(i\beta_1^2(j)) + \xi_{21}(j), \tag{A9}$$

$$\begin{pmatrix} \frac{\partial \xi(j)}{\partial \gamma(j)} \\ \frac{\partial \xi_1(j)}{\partial \xi_{10}(j)} \end{pmatrix} = \begin{pmatrix} \frac{s(\frac{|p_1|^2(j)-1}{|p_1|(j)}\;\frac{\partial |p_1|^2(j)}{\partial \gamma(j)} - 4(1+|p_1|^2(j))|p_1|(j)\pi\beta_1(j)\frac{\partial \beta_1(j)}{\partial \gamma(j)})}{2|p_1|(j)(4|p_1|^2(j)e^{2\pi\beta_1^2(j)} - (1+|p_1|^2(j))^2)^{1/2}} \\ \frac{s(\frac{|p_1|^2(j)-1}{|p_1|(j)}\;\frac{\partial |p_1|^2(j)}{\partial \xi_{10}(j)} - 4(1+|p_1|^2(j))|p_1|(j)\pi\beta_1(j)\frac{\partial \beta_1(j)}{\partial \xi_{10}(j)})}{2|p_1|(j)(4|p_1|^2(j)e^{2\pi\beta_1^2(j)} - (1+|p_1|^2(j))^2)^{1/2}} \end{pmatrix}, \tag{A10}$$

$$\begin{pmatrix} \dfrac{\partial\gamma_1(j)}{\partial\gamma(j)} & \dfrac{\partial\gamma_1(j)}{\partial\xi_{10}(j)} \\ \dfrac{\partial\xi_{11}(j)}{\partial\gamma(j)} & \dfrac{\partial\xi_{11}(j)}{\partial\xi_{10}(j)} \end{pmatrix} \tag{A11}$$

with

$$\frac{\partial\gamma_1(j)}{\partial\gamma(j)} = \frac{\partial|p_1|^2(j)/\partial\gamma(j)}{2\pi\gamma_1(j)(1+|p_1|^2(j))} ,$$

$$\frac{\partial\xi_{11}(j)}{\partial\gamma(j)} = \frac{\partial\gamma_1(j)}{\partial\gamma(j)}\left(3\gamma_1(j)\ln 2 - \gamma_1(j)\mathrm{Re}\,\psi\left(1+\frac{i\gamma_1^2(j)}{2}\right)\right) - \frac{\partial\xi_1(j)}{\partial\gamma(j)} ,$$

$$\frac{\partial\gamma_1(j)}{\partial\xi_{10}(j)} = \frac{\partial|p_1|^2(j)/\partial\xi_{10}(j)}{2\pi\gamma_1(j)(1+|p_1|^2(j))} ,$$

$$\frac{\partial\xi_{11}(j)}{\partial\xi_{10}(j)} = \frac{\partial\gamma_1(j)}{\partial\xi_{10}(j)}\left(3\gamma_1(j)\ln 2 - \gamma_1(j)\mathrm{Re}\,\psi\left(1+\frac{i\gamma_1^2(j)}{2}\right)\right) - \frac{\partial\xi_1(j)}{\partial\xi_{10}(j)} .$$

Using (A5)–(A11) we finally arrive at the following Jacobian of the Poincaré map:

$$\begin{pmatrix} \dfrac{\partial\gamma(j+1)}{\partial\gamma(j)} & \dfrac{\partial\gamma(j+1)}{\partial\xi_{10}(j)} \\ \dfrac{\partial\xi_{10}(j+1)}{\partial\gamma(j)} & \dfrac{\partial\xi_{10}(j+1)}{\partial\xi_{10}(j)} \end{pmatrix} \tag{A12}$$

with

$$\frac{\partial\gamma(j+1)}{\partial\gamma(j)} = e^{-k\pi/2}\frac{\partial\gamma_1(j)}{\partial\gamma(j)} ,$$

$$\frac{\partial\xi_{10}(j+1)}{\partial\gamma(j)} = \frac{3}{2}\,\gamma_2(j)g_1(k)\frac{\partial\gamma_1(j)}{\partial\gamma(j)} - \frac{\partial\xi_{11}(j)}{\partial\gamma(j)} ,$$

$$\frac{\partial\gamma(j+1)}{\partial\xi_{10}(j)} = e^{-k\pi/2}\frac{\partial\gamma_1(j)}{\partial\xi_{10}(j)} ,$$

$$\frac{\partial\xi_{10}(j+1)}{\partial\xi_{10}(j)} = \frac{3}{2}\,\gamma_1(j)g_2(k)\frac{\partial\gamma_1(j)}{\partial\xi_{10}(j)} - \frac{\partial\xi_{11}(j)}{\partial\xi_{10}(j)} .$$

References

1. Guckenheimer, J. and Holmes, P., *Nonlinear Oscillations, Dynamical Systems, and Bifurcations of Vector Fields*, Springer-Verlag, New York, 1983.
2. Its, A. R., Fokas, A. S., and Kapaev, A. A., 'On the asymptotic analysis of the Painlevé equations via the isomonodromy method', *Nonlinearity* **7**, 1994, 1291–1325.
3. Lichtenberg, A. J. and Lieberman, M. A., *Regular and Stochastic Motion*, Springer-Verlag, Berlin, 1983.

4. Bridge, J. and Rand, R. H., 'Chaos and symbol sequences in systems with a periodically disappearing figure-eight separatrix', in *Proceedings of 1992 ASME Bifurcation Phenomena and Chaos in Thermal Convection*, Vol. 214, 1992, pp. 47–55.
5. Coppola, V. T. and Rand, R. H., 'Computer algebra, elliptic functions and chaos', in *Proceedings of 1990 ASME International Computers in Engineering Conference*, Vol. 1, Boston, MA, August 6–10, 1990, pp. 193–200.
6. Coppola, V. T. and Rand, R. H., 'Chaos in a system with a periodically disappearing separatrix', *Nonlinear Dynamics* **1**, 1990, 401–420.
7. Eckhaus, W., *Asymptotic Analysis of Singular Perturbations*, North-Holland, Amsterdam/New York/Oxford, 1979.
8. Verhulst, F., *Nonlinear Differential Equations and Dynamical Systems*, Springer-Verlag, Berlin, 1990.
9. Sanders, J. A. and Verhulst, F., *Averaging Methods in Nonlinear Dynamical Systems*, Springer-Verlag, New York, 1985.
10. Bourland, F. J. and Haberman, R., 'Separatrix crossing: Time-invariant potentials with dissipation', *SIAM Journal of Applied Mathematics* **50**, 1990, 1716–1744.
11. Neihstadt, A. I., 'Passage through a separatrix in a resonance problem with a slowly-varying parameter', *Journal of Applied Mathematics and Mechanics (PMM)* **39**, 1975, 594–605.
12. Bosley, D. L. and Kevorkian, J., 'Sustained resonance in very slowly varying oscillatory Hamiltonian systems', *SIAM Journal of Applied Mathematics* **52**, 1992, 494–527.
13. Marée, G. J. M., 'Sudden change in a second-order non-linear system with a slowly varying parameter', *International Journal of Non-Linear Mechanics* **28**, 1993, 409–426.
14. Kaper, T. J. and Wiggins, S., 'Lobe area in adiabatic Hamiltonian systems', *Physica D* **51**, 1991, 205–212.
15. Haberman, R., 'Slowly varying jump and transition phenomena associated with algebraic bifurcation problems', *SIAM Journal of Applied Mathematics* **37**, 1979, 69–106.
16. Abramowitz, M. and Stegun, I. A., *Handbook of Mathematical Functions*, National Bureau of Standards, Washington, DC, 1964.
17. Marée, G. J. M., 'Slow passage through a pitchfork bifurcation', *SIAM Journal of Applied Mathematics* **56**, 1996, 889–918.
18. Ott, E., *Chaotic Dynamics*, Cambridge University Press, Cambridge, 1993.